

Accelerating delayed-acceptance Markov chain Monte Carlo algorithms

Samuel Wiqvist^{*}, Umberto Picchini^{◇*}, Julie Lyng Forman[†]

^{*}Centre for Mathematical Sciences, Lund University, Sweden

[◇]Department of Mathematical Sciences, Chalmers University of Technology and the University of Gothenburg, Sweden

[†]Dept. Public Health, section of Biostatistics, University of Copenhagen, Denmark

Abstract

Delayed-acceptance Markov chain Monte Carlo (DA-MCMC) samples from a probability distribution, via a two-stages version of the Metropolis-Hastings algorithm, by combining the target distribution with a “surrogate” (i.e. an approximate and computationally cheaper version) of said distribution. DA-MCMC accelerates MCMC sampling in complex applications, while still targeting the *exact* distribution. We design a computationally faster DA-MCMC algorithm, which samples from an *approximation* of the target distribution. As a case study, we also introduce a novel stochastic differential equation model for protein folding data. We consider parameters inference in a Bayesian setting where a surrogate likelihood function is introduced in the delayed-acceptance scheme. In our applications we employ a Gaussian process as a surrogate likelihood, but other options are possible. In our accelerated algorithm the calculations in the “second stage” of the delayed-acceptance scheme are reordered in such a way that we can obtain a significant speed-up in the MCMC sampling, when the evaluation of the likelihood function is computationally intensive. We consider both simulation studies, and the analysis of real protein folding data. Simulation studies for the stochastic Ricker model and the novel stochastic differential equation model for protein-folding data, show that the speed-up is highly problem dependent. The more involved the computations of the likelihood function are, the higher the acceleration becomes when using our algorithm. Inference results for the standard delayed-acceptance algorithm and our approximated version are similar, indicating that our approximated algorithm can return reliable Bayesian inference.

Keywords: Bayesian inference, Gaussian process, pseudo marginal MCMC, protein folding, stochastic differential equation

1 Introduction

In this work we introduce a new algorithm for Bayesian inference, proposing ways to accelerate Markov chain Monte Carlo (MCMC) sampling when the evaluation of the target distribution is computationally expensive. We build on the “delayed-acceptance” (DA) strategy developed in [Christen and Fox \[2005\]](#) where a fast, “two-stages” DA-MCMC algorithm is proposed while still targeting the desired distribution exactly. We produce an approximated and accelerated delayed acceptance MCMC algorithm (ADA-MCMC), where in exchange of exactness we are returned with results even more rapidly than the standard DA-MCMC.

More in detail, we aim at sampling from the posterior distribution $p(\theta|y) \propto p(y|\theta)\pi(\theta)$ where θ are model parameters, y denotes data, $p(y|\theta)$ is the likelihood function, and $\pi(\theta)$ is the prior distribution of θ . We assume that the point-wise evaluation of the likelihood $p(y|\theta)$ (or an approximation thereof) is computationally intensive, because the underlying probabilistic model is complex and/or

the data y is large. For those situations DA-MCMC algorithms turn particularly useful. In the approach originally outlined in [Christen and Fox \[2005\]](#), which is not specified for Bayesian inference but is more generally applicable for sampling from generic distributions, a DA strategy decomposes an MCMC move into two stages. At the first stage a proposal can either be rejected, according to a “surrogate of the posterior” (one that is computationally cheap to evaluate and chosen to approximate the desired posterior), or be sent to the second stage. If the proposal is not rejected at the first stage, at the second stage an acceptance probability is used that corrects for the discrepancy between the approximate surrogate and the desired posterior, and at this stage the proposal can finally be accepted or rejected. The advantage of using DA-MCMC is that the computationally expensive posterior only appears in the second stage, whereas the surrogate posterior in the first stage is cheap to evaluate. Therefore, in the first stage the surrogate posterior rapidly screens proposals, and rejects those that are unlikely to be accepted at the second stage, if the surrogate model is reliable. Our approach is described with focus on Bayesian inference (though we also show that this is not a limitation and it can be used for sampling from generic distributions), and we build a surrogate of the computationally expensive likelihood function, while we assume the cost of evaluating the prior to be negligible. Therefore the expensive likelihood appears only in the second stage. Some implementations of the DA approach in Bayesian inference can be found e.g. in [Golightly et al. \[2015\]](#), [Sherlock et al. \[2017\]](#), and [Banterle et al. \[2015\]](#), and similar approaches based on approximate Bayesian computation (ABC) can be found in [Picchini \[2014\]](#), [Picchini and Forman \[2016\]](#), and [Everitt and Rowińska \[2017\]](#).

In this work, the sequence of computations pertaining the second stage of DA-MCMC are arranged so to find opportunities to avoid the evaluation of the expensive likelihood. This leads to our accelerated and approximated ADA-MCMC. Therefore, the benefit of using ADA-MCMC is that, unlike DA-MCMC, once a parameter proposal reaches the second stage, the expensive likelihood is not necessarily evaluated, but this comes at the price of introducing an approximation in the sampling procedure. We test and compare delayed-acceptance algorithms, particle marginal methods for exact Bayesian inference, and Markov-chain-within-Metropolis on two case studies, one of which considers a novel state-space model for protein folding data, with dynamics expressed via a stochastic differential equation (SDE). Therefore, in this work we contribute with: (i) a novel, approximate and accelerated delayed-acceptance MCMC algorithm, and (ii) a novel double-well potential state-space model for protein folding data. For practical applications, we use Gaussian processes to specify surrogates of the likelihood function, though this is not an essential component of our approach and other surrogates of the likelihood can be considered. We found that the acceleration produced by ADA-MCMC, compared to DA-MCMC, is dependent on the specific application. If the exact or approximate likelihood function used in the second stage of the algorithm is not computationally very intensive to evaluate, then our method produces negligible benefits. Therefore the use of our ADA-MCMC, just as the standard DA-MCMC, is beneficial when each evaluation of the likelihood has a non-negligible impact on the total computational budget. Then, the time savings due to ADA-MCMC are proportional to the number of MCMC iterations where the evaluation of the likelihood at the second stage is avoided. In terms of inference quality, we find that ADA-MCMC returns results that are very close to DA-MCMC, so our approximations do not seem to harm the accuracy of the resulting inference.

The outline of this paper is as follows: The delayed-acceptance scheme and our novel accelerated delayed-acceptance algorithm are introduced in a general framework in [Section 2](#). In [Section 3](#) the properties of the particle Markov chain Monte Carlo, and the closely related Markov-chain-within-Metropolis algorithms are discussed. The Gaussian process surrogate model is introduced in [Section 4](#), and the delayed-acceptance Gaussian process MCMC and accelerated delayed-acceptance Gaussian process MCMC algorithm are introduced in [Section 5](#). [Section 6](#) contains information regarding the implementations of the algorithms. The simulation study for the stochastic Ricker model is in [Section 7.1](#). The protein folding data and the novel double-well potential stochastic differential equation model are introduced in [Section 7.2](#). A discussion in [Section 8](#) closes our work. Further supplementary material is available, and the code used to generate results can be found at

2 Delayed-acceptance MCMC

We first introduce the delayed-acceptance (DA-MCMC) scheme due to [Christen and Fox \[2005\]](#) in full generality, then we specialize it for Bayesian inference, and finally our accelerated delayed-acceptance (ADA-MCMC) algorithm is introduced in section 2.1. In this section we consider a very general framework. However we anticipate that, for the case studies, we employ Gaussian processes as surrogate models of the likelihood function, as detailed in Section 4, and the corresponding delayed-acceptance Gaussian process MCMC (DA-GP-MCMC) and accelerated delayed-acceptance Gaussian process MCMC (ADA-GP-MCMC) algorithms are discussed in Section 5.

In a general framework, we are interested in sampling from some distribution $p(x)$ using the Metropolis-Hastings algorithm [[Hastings, 1970](#)]. Metropolis-Hastings proceeds by evaluating whether accepting or rejecting random moves produced by a Markov kernel from the current value of x to a new x^* . The sequence of accepted moves forms a Markov chain having $p(x)$ as stationary distribution. Now assume that the point-wise evaluation of $p(x)$ is computationally expensive. The main idea behind a DA-MCMC approach is to delay (or avoid as much as possible) the evaluation of the computationally expensive $p(x)$, by first trying to early-reject the proposal x^* using some surrogate (cheap to evaluate) deterministic or stochastic model $\tilde{p}(x)$. To enable early-rejections while still targeting the distribution $p(x)$, a two-stages acceptance scheme is introduced in [Christen and Fox \[2005\]](#). Say that we are at the r th iteration of the Metropolis-Hastings algorithm, and denote with x^{r-1} the state of the chain produced at the previous iteration. Then at first stage of DA-MCMC we evaluate the “acceptance probability” (we use quotes as at this stage we do not really accept any proposal)

$$\alpha_1 = \min\left(1, \frac{\tilde{p}(x^*)}{\tilde{p}(x^{r-1})} \cdot \frac{g(x^{r-1}|x^*)}{g(x^*|x^{r-1})}\right), \quad (1)$$

where $g(x|y)$ is the transition kernel used to generate proposals, i.e. at the r th iteration $x^* \sim g(x|x^{r-1})$. If the proposal x^* “survives” the first stage (i.e. if it is not rejected) it is then sent to the second stage where it is accepted with probability α_2

$$\alpha_2 = \min\left(1, \frac{p(x^*)}{p(x^{r-1})} \cdot \frac{\tilde{p}(x^{r-1})}{\tilde{p}(x^*)}\right). \quad (2)$$

Therefore x^* can only be accepted at the second stage, while it can be rejected both at the first and second stage. A computational speed-up is obtained when x^* is early-rejected at the first stage, as there the expensive $p(x^*)$ is not evaluated. Hence, to obtain a significant speed-up it is important to be able to early-reject those proposals which will be likely rejected at the second stage. Or, in other words, a proposal is first “tested” at the first stage and then it is sent to the second stage only if this is not unlikely to be accepted. The probability α_2 corrects for the approximation introduced in the first stage and [Christen and Fox \[2005\]](#) prove that the resulting Markov chain has the correct stationary distribution p . This result holds if g is p -irreducible and reversible, and if $g(x|y) > 0$ implies $\tilde{p}(x) > 0$. From (2) it is evident how the surrogate model acts as a proposal distribution. See [Franks and Vihola \[2017\]](#) for a comparison in terms of asymptotic variances of Monte Carlo estimators provided via importance sampling, pseudo-marginal and delayed-acceptance methods.

In a Bayesian framework we are interested in sampling from the posterior distribution $p(\theta|y) \propto p(y|\theta)\pi(\theta)$. Furthermore, for the cases of interest to us the log-likelihood function, or an approximation thereof $\ell(\theta) := \log p(y|\theta)$, is computationally expensive while the prior distribution is assumed cheap to evaluate. By introducing a deterministic or stochastic surrogate log-likelihood $\tilde{\ell}(\theta)$, the DA algorithm can be used to early-reject proposals θ^* that are unlikely to be accepted. In this case the first stage acceptance probability is

$$\alpha_1 = \min\left(1, \frac{\tilde{\ell}(\theta^*)}{\tilde{\ell}(\theta^{r-1})} \cdot \frac{\pi(\theta^*)}{\pi(\theta^{r-1})} \cdot \frac{g_1(\theta^{r-1}|\theta^*)}{g_1(\theta^*|\theta^{r-1})}\right),$$

where g_1 is the transition kernel, and the surrogate likelihood is $\tilde{L}(\theta) := \exp(\tilde{\ell}(\theta))$. Similarly, by setting $L(\theta) := \exp(\ell(\theta))$, the second stage acceptance probability is

$$\alpha_2 = \min\left(1, \frac{L(\theta^*)}{L(\theta^{r-1})} \cdot \frac{\tilde{L}(\theta^{r-1})}{\tilde{L}(\theta^*)}\right).$$

An extension of the DA-MCMC scheme due to [Sherlock et al. \[2017\]](#) is to generate a proposal θ^* from a different transition kernel $g_2(\cdot|\theta^{r-1})$, and with a small but positive probability $\beta_{MH} \in (0, 1)$ allow the evaluation of the proposal θ^* in an ordinary Metropolis-Hastings algorithm, with acceptance probability denoted α_{MH} ,

$$\alpha_{MH} = \min\left(1, \frac{L(\theta^*)}{L(\theta^{r-1})} \cdot \frac{\pi(\theta^*)}{\pi(\theta^{r-1})} \cdot \frac{g_2(\theta^{r-1}|\theta^*)}{g_2(\theta^*|\theta^{r-1})}\right). \quad (3)$$

In this case the proposal can be immediately accepted or rejected as in a regular MCMC. The transition kernel g_1 should have a somewhat larger variance than the transition kernel g_2 . With probability $1 - \beta_{MH}$ a proposal is instead evaluated using the two-stages of a DA-MCMC algorithm.

When using this “extended version” of DA-MCMC (where a β_{MH} is introduced), since the delayed-acceptance stage is skipped with probability β_{MH} , it is preferable to use a small β_{MH} in order not to lose too much of the acceleration implied by a delayed-acceptance approach. Our experience also indicates that this extension can be critical to better explore the tails of the posterior distribution, compared to a standard DA-MCMC (which is obtained when $\beta_{MH} = 0$). This “mixture” of the two Metropolis-Hastings kernels (i.e. the acceptance kernel for the DA scheme, and the acceptance kernel in (3)) indeed produce a valid MCMC algorithm since both kernels in the standard cases target the correct posterior distribution [[Rosenthal and Roberts, 2007](#)].

2.1 Accelerated delayed-acceptance MCMC

There have been a number of attempts at accelerating the original DA-MCMC of [Christen and Fox \[2005\]](#). For example, in a Bayesian framework, [Banterle et al. \[2015\]](#) propose to break down the posterior into the product of d chunks. The Metropolis-hastings acceptance ratio becomes the product of d acceptance ratios, each of which can be sequentially evaluated against one of d independent uniform variates. The acceleration is given by the possibility to “early-reject” a proposal, as soon as one of those d acceptance ratios leads to a rejection (in the same spirit of [Solonen et al., 2012](#)). However, an acceptance instead requires scanning all d components, i.e. the full posterior. [Quiroz et al. \[2017\]](#) never use the full data set in the second stage of DA and instead construct an approximated likelihood from subsamples of the data, which is particularly relevant for BigData problems (see references therein and [Angelino et al. \[2016\]](#) for further discussion on subsampling methods). Remarkably, [Quiroz et al. \[2017\]](#) prove that even when the full likelihood is approximated using data subsamples, the resulting chain has the correct stationary distribution as if the full data set was employed. However, they assume data to be conditionally independent, a strong condition which does not apply to case studies considered in the present work.

We now introduce the novel accelerated delayed-acceptance DA-MCMC algorithm, shortly ADA-MCMC. The main idea behind ADA-MCMC is that, under some assumptions on how the likelihood function and the surrogate model relate, it is possible to arrange the computations in the second stage of the DA algorithm to obtain an acceleration in the computations. This is implied by the possibility to avoid the evaluation of the expensive likelihood in the second stage, in some specific circumstances. However, this also implies that ADA-MCMC is an approximated procedure, since a proposal can sometimes be accepted according to the surrogate model. We introduce ADA-MCMC in a Bayesian setting where the surrogate model pertains the log-likelihood function. However, the idea can straightforwardly be adapted to the case where a surrogate model of a generic distribution $p(x)$ is used, as in equations (1)-(2). The more general setting is briefly described later in this section.

As previously mentioned, at the r th iteration the DA algorithm is governed by the values of the likelihood function $L(\theta^*)$ and $L(\theta^{r-1})$, and the values of the surrogate model $\tilde{L}(\theta^*)$ and $\tilde{L}(\theta^{r-1})$. These four values can be considered in four mutually exclusive scenarios:

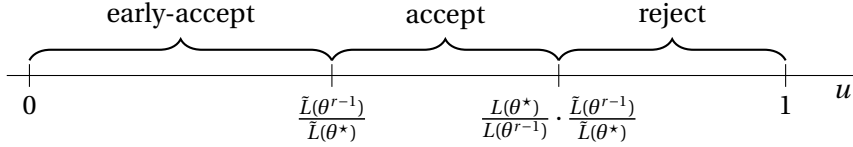
- 1) $\tilde{L}(\theta^*) > \tilde{L}(\theta^{r-1})$ and $L(\theta^*) > L(\theta^{r-1})$,
- 2) $\tilde{L}(\theta^*) < \tilde{L}(\theta^{r-1})$ and $L(\theta^*) < L(\theta^{r-1})$,
- 3) $\tilde{L}(\theta^*) > \tilde{L}(\theta^{r-1})$ and $L(\theta^*) < L(\theta^{r-1})$,
- 4) $\tilde{L}(\theta^*) < \tilde{L}(\theta^{r-1})$ and $L(\theta^*) > L(\theta^{r-1})$.

We study each of the four cases separately to investigate any opportunity for accelerating the computations in the second stage of DA-MCMC, under the assumption that the relations between the evaluations of \tilde{L} and L hold. Afterwards, we suggest ways to determine approximately which of the four possibilities we should assume to hold, for any new proposal θ^* , without evaluating the expensive likelihood $L(\theta^*)$.

Case 1) Under the assumption that $\tilde{L}(\theta^*) > \tilde{L}(\theta^{r-1})$ and $L(\theta^*) > L(\theta^{r-1})$ it is clear that $\frac{\tilde{L}(\theta^{r-1})}{\tilde{L}(\theta^*)} < 1$ and $\frac{L(\theta^{r-1})}{L(\theta^*)} < 1$. It also holds that

$$\frac{\tilde{L}(\theta^{r-1})}{\tilde{L}(\theta^*)} < \frac{L(\theta^*)}{L(\theta^{r-1})} \cdot \frac{\tilde{L}(\theta^{r-1})}{\tilde{L}(\theta^*)}. \quad (4)$$

Hence, the acceptance region for the second stage can be split in two parts where one part is “governed” by $\frac{\tilde{L}(\theta^{r-1})}{\tilde{L}(\theta^*)}$ only. To clarify, at the second stage of the standard DA-MCMC introduced previously, acceptance of a proposed θ^* takes place if $u < \frac{L(\theta^*)}{L(\theta^{r-1})} \cdot \frac{\tilde{L}(\theta^{r-1})}{\tilde{L}(\theta^*)}$ where u is uniformly distributed in $[0,1]$, hence, the acceptance region is $[0, \frac{L(\theta^*)}{L(\theta^{r-1})} \cdot \frac{\tilde{L}(\theta^{r-1})}{\tilde{L}(\theta^*)}]$. However, because of (4) we are allowed to further decompose the acceptance region, as presented below:



Hence, if a proposal θ^* has survived the first stage and we assume that we are in case 1, we can *first* check whether we can “early-accept” the proposal (i.e. without evaluating the expensive likelihood), that is, check if

$$u < \frac{\tilde{L}(\theta^{r-1})}{\tilde{L}(\theta^*)}, \quad (5)$$

and if this is the case θ^* is (early)-accepted and stored, and we can move to the next iteration of ADA-MCMC. If θ^* is not early-accepted, we can look into the remaining part of the $[0,1]$ segment to determine if the proposal can be accepted or rejected. Hence, when early-acceptance is not possible, the expensive likelihood $L(\theta^*)$ is evaluated and the proposal is accepted and stored if

$$u < \frac{L(\theta^*)}{L(\theta^{r-1})} \cdot \frac{\tilde{L}(\theta^{r-1})}{\tilde{L}(\theta^*)}, \quad (6)$$

and rejected otherwise, and we can move to the next iteration of ADA-MCMC.

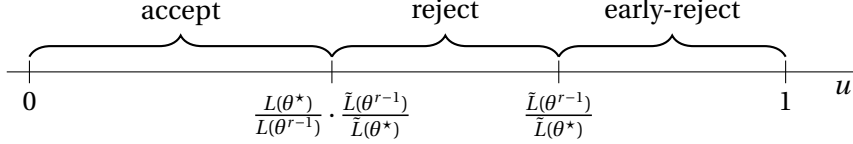
Since the acceptance region for the second stage is split in two parts (early-acceptance and acceptance), the *same* random number u is used in (5) and (6). By splitting the region it is possible to early-accept proposals without evaluating $L(\theta^*)$, and thereby obtaining a speed-up.

Case 2) If this case holds, then $\frac{\tilde{L}(\theta^{r-1})}{\tilde{L}(\theta^*)} > 1$ and $\frac{L(\theta^*)}{L(\theta^{r-1})} < 1$. Hence, it is not possible to obtain any early-accept or early-reject opportunities in this case.

Case 3) If this case holds, then $\frac{\tilde{L}(\theta^{r-1})}{\tilde{L}(\theta^*)} < 1$ and $\frac{L(\theta^*)}{L(\theta^{r-1})} < 1$. Hence, it also holds that

$$\frac{\tilde{L}(\theta^{r-1})}{\tilde{L}(\theta^*)} > \frac{L(\theta^*)}{L(\theta^{r-1})} \cdot \frac{\tilde{L}(\theta^{r-1})}{\tilde{L}(\theta^*)}.$$

The rejection region is $[\frac{L(\theta^*)}{L(\theta^{r-1})} \cdot \frac{\tilde{L}(\theta^{r-1})}{\tilde{L}(\theta^*)}, 1]$ and this can be split-up into two parts, where one part is only governed by $\frac{\tilde{L}(\theta^{r-1})}{\tilde{L}(\theta^*)}$, see below:



By simulating a draw u uniformly in $[0,1]$, we can first check if the proposal can be early-rejected. This happens if

$$u > \frac{\tilde{L}(\theta^{r-1})}{\tilde{L}(\theta^*)}.$$

If the proposal is not early-rejected, it is accepted if

$$u < \frac{L(\theta^*)}{L(\theta^{r-1})} \cdot \frac{\tilde{L}(\theta^{r-1})}{\tilde{L}(\theta^*)},$$

and rejected otherwise. Hence, in case 3 there is a chance to early-reject a proposed θ^* without evaluating $L(\theta^*)$.

Case 4) Under the assumption we have that $\frac{\tilde{L}(\theta^{r-1})}{\tilde{L}(\theta^*)} > 1$ and $\frac{L(\theta^*)}{L(\theta^{r-1})} > 1$, and we can immediately accept the proposal without evaluating $L(\theta^*)$, since $\frac{L(\theta^*)}{L(\theta^{r-1})} \cdot \frac{\tilde{L}(\theta^{r-1})}{\tilde{L}(\theta^*)} > 1$.

As previously mentioned, some of the cases described above allow for an early rejection or an early acceptance solely based on the ratio of the surrogate likelihoods. Moreover, assuming a specific case to be the “right one”, for proposal θ^* , is a decision subject to a probabilistic error. This is why ADA-MCMC is an approximate version of DA-MCMC. Clearly, the crucial problem is to determine which of the four cases to assume to hold for proposal θ^* . One method is to consider a pre-run of *some* MCMC algorithm to estimate the probability for each of the four different cases ($\hat{p}_1, \hat{p}_2, \hat{p}_3, \hat{p}_4$), where p_j is the true but unknown probability that case j holds, $j = 1, \dots, 4$. This is of course a possibly computationally heavy procedure, however, for the specific algorithms we study in section 5, such a pre-run is necessary to construct the surrogate model for the log-likelihood, hence the estimation of the p_j 's comes as a simple by-product of the inference procedure. Then, once the \hat{p}_j 's are obtained, for a new θ^* one first check if $\frac{\tilde{L}(\theta^{r-1})}{\tilde{L}(\theta^*)} < 1$ or if $\frac{\tilde{L}(\theta^{r-1})}{\tilde{L}(\theta^*)} > 1$. If $\frac{\tilde{L}(\theta^{r-1})}{\tilde{L}(\theta^*)} > 1$ then we toss a uniform u and if $u < \hat{p}_2$ case 2 is selected with probability \hat{p}_2 (and case 4 is selected with probability $\hat{p}_4 = 1 - \hat{p}_2$). Correspondingly, if $\frac{\tilde{L}(\theta^{r-1})}{\tilde{L}(\theta^*)} < 1$ then we toss a uniform u and if $u < \hat{p}_1$ case 1 is selected with probability \hat{p}_1 (and case 3 is selected with probability $\hat{p}_3 = 1 - \hat{p}_1$). Another approach is to model the probabilities as a function of θ . Hence, we are then interested in computing the probabilities $\hat{p}_1(\theta)$, $\hat{p}_2(\theta)$, $\hat{p}_3(\theta)$, and $\hat{p}_4(\theta)$. For this task, we can for instance use logistic regression, or some other classification algorithm to select which case to assume. The problem of the selection of cases 1–4 is discussed in detail in Section 5.1, where explicit suggestions are given for the algorithms we introduce in that section.

In Section 3 we introduce models and algorithms that, although not strictly necessary for the ADA-MCMC approach, constitute an important framework for intractable-likelihoods problems in

Bayesian inference. These are the “pseudo-marginal” particle MCMC algorithms, that have found important applications in inference for state-space models (though not limited to this class of models). We briefly discuss pseudo-marginal methods and state-space models, then in Section 5 we specialize ADA-MCMC to accelerate pseudo-marginal algorithms.

We stated early that ADA can also be used in a non-Bayesian setting, where we target a generic distribution $p(x)$ for some $x \in \mathcal{X}$. In that case we need to introduce a corresponding surrogate model $\tilde{p}(x)$. The r th iteration of ADA will then be governed by the four values $\tilde{p}(x^*)$, $\tilde{p}(x^{r-1})$, $p(x^*)$, and $p(x^{r-1})$, where x^* is a proposed value $x^* \in \mathcal{X}$. These can be arranged into four cases, similarly to what previously described:

- 1) $\tilde{p}(x^*) > \tilde{p}(x^{r-1})$ and $p(x^*) > p(x^{r-1})$,
- 2) $\tilde{p}(x^*) < \tilde{p}(x^{r-1})$ and $p(x^*) < p(x^{r-1})$,
- 3) $\tilde{p}(x^*) > \tilde{p}(x^{r-1})$ and $p(x^*) < p(x^{r-1})$,
- 4) $\tilde{p}(x^*) < \tilde{p}(x^{r-1})$ and $p(x^*) > p(x^{r-1})$.

Therefore, by adapting the methodology, possibilities for early-rejection and early-acceptance of a proposal x^* can straightforwardly be obtained regardless of whether we pursue a Bayesian analysis or not.

3 Particle marginal methods for state-space models

The challenge of approximating the likelihood function for complex models with “intractable likelihoods” has generated a large body of literature in the past fifteen years, most notably approximate Bayesian computation (ABC, see the reviews [Sisson and Fan, 2011](#) and [Karabatsos and Leisen, 2017](#)) and pseudo-marginal (particle) MCMC algorithms ([Beaumont, 2003](#), [Andrieu and Roberts, 2009](#), [Andrieu et al., 2010](#)). Pseudo-marginal algorithms in particular have found an immediate success in inference for state-space models using sequential Monte Carlo (or particle filters); reviews are [Jacob \[2015\]](#) and [Kantas et al. \[2015\]](#). We illustrate our accelerated delayed-acceptance MCMC on case studies using the pseudo-marginal approach. However, pseudo-marginal methods are not a requirement to exploit ADA-MCMC, but rather an important application of the method.

Pseudo-marginal algorithms build on the interplay between Markov chain Monte Carlo (MCMC), importance sampling and sequential Monte Carlo (SMC, or particle filters) algorithms. The crucial result is that when the likelihood $p(y|\theta)$ is not available analytically but obtaining a non-negative unbiased estimator $\hat{p}(y|\theta)$ is possible, then a Metropolis-Hastings algorithm using $\hat{p}(y|\theta)$ instead of $p(y|\theta)$ will generate a Markov chain having $p(\theta|y)$ as stationary distribution. This means that it is possible to target the exact posterior even when we deal with an (unbiased) approximation to the likelihood function, rather than the exact likelihood. [Andrieu and Roberts \[2009\]](#) discuss the problem by estimating unbiasedly the unavailable likelihood using N draws from an importance sampler, and the remarkable result is once more that exact Bayesian sampling from $p(\theta|y)$ is possible for any finite value of N . [Andrieu et al. \[2010\]](#) frame their particle MCMC (PMCMC) approach for a large class of statistical models, including state-space models (SSM, [Cappé et al., 2005](#)). For SSM an unbiased estimator $\hat{p}(y|\theta)$ is given by particle filters using N particles (here and in the following we write $\hat{p}(y|\theta) \equiv \hat{p}_N(y|\theta)$ since the resulting inference for θ is theoretically unaffected by the value of N). In [Andrieu et al. \[2010\]](#) the PMCMC algorithms PMMH (particle marginal Metropolis-Hastings) and PG (particle Gibbs) target the posterior $p(\theta, x_{1:T}|y_{1:T})$ exactly, where $y_{1:T}$ is the sequence of measurements from process $\{y_t\}$ in (7) collected at T discrete times which, to simplify the notation, we assume to be the integers $\{1, 2, \dots, T\}$. With $x_{1:T}$ we denote the corresponding latent (unobservable) dynamics, see (7). We employ the following notation for sequences of variables $z_{1:T} \equiv \{z_1, \dots, z_T\}$. Therefore PMMH and PG solve simultaneously the parameter inference and the state filtering problem. In the next sections we clarify how these pseudo-marginal methods (PMM) and the delayed-acceptance (DA) framework interact, while emphasizing once more that in order to run a DA algorithm, including our accelerated DA method, the PMM framework is not necessary, nor is our methodology specific for dynamic models such as SSM but can be applied also to “static” models.

A SSM can be written as

$$\begin{cases} y_t \sim p(y_t|x_t;\theta_y) \\ x_t \sim p(x_t|x_s,\theta_x), \quad x_0 \sim p(x_0), \quad t_0 \leq s < t, \end{cases} \quad (7)$$

where $x_0 \equiv x_{t_0}$ is a random initial state with initial distribution $p(x_0)$, observations $y_t \in \mathbb{R}^{d_y}$ depend on a finite dimensional unknown parameter θ_y , and observations are conditionally independent given the latent state $\{x_t\}_{t \geq t_0}$, with $x_t \in \mathbb{R}^{d_x}$, and $d_x, d_y \geq 1$. Here $\{x_t\}$ is a continuous Markov process equipped with a transition density $p(x_t|x_s, \cdot)$ for $s < t$ and depending on another finite dimensional unknown parameter θ_x . Therefore we have that $\theta = (\theta_x, \theta_y)$ is the parameter object of our inference. In this work we consider posterior inference for θ , hence our ideal target is $p(\theta|y_{1:T})$, however, instead of calling the algorithms “pseudo-marginal”, we call them PMCMC, since we use particle filters to approximate the likelihood function. But recall that we are not interested in the filtering problem for $x_{1:T}$.

Despite the existence of these powerful and flexible algorithms, computing an (unbiased) estimator of the likelihood function can be computationally time-consuming for complex models. Computationally cheap surrogate models have therefore been used to accelerate instances of the PMCMC algorithm. As an example, in [Drovandi et al. \[2018\]](#) a surrogate model based on Gaussian processes (GP) is used to replace the time-consuming sequential Monte Carlo estimation of the likelihood function. After an initial, computationally expensive “training phase”, a GP regression model is fitted to the output of the training phase (consisting of proposed parameter values and log-likelihoods estimated via particle filters), and the estimated GP is then used as a (cheap) surrogate of the log-likelihood function, allowing for considerable computational acceleration in the MCMC sampling.

Another approach is to not entirely replace the sequential Monte Carlo estimation of the likelihood function, but only compute these estimations for parameter proposals that are not “early-rejected” by the surrogate model. This is a delayed-acceptance (DA) approach, used for example in [Golightly et al. \[2015\]](#) and [Sherlock et al. \[2017\]](#). As already mentioned, DA-MCMC has two important properties: the ergodicity of the chain is preserved, and the resulting Markov chain targets the true posterior distribution of θ . In [Golightly et al. \[2015\]](#) the surrogate model is based on Langevin diffusion approximations and linear noise approximations. In [Sherlock et al. \[2017\]](#) the surrogate estimation of the likelihood function is computed using previous estimations via a search-tree. Hence, quite different surrogate models can be employed and still resulting in an valid DA-MCMC for exact Bayesian inference.

3.1 Particle Markov chain Monte Carlo

The likelihood function for the SSM (7) can be written as

$$p(y_{1:T}|\theta) = p(y_1|\theta) \prod_{t=2}^T p(y_t|y_{1:t-1};\theta)$$

where

$$p(y_t|y_{1:t-1};\theta) = \int p(y_t|x_t;\theta) p(x_t|y_{1:t-1};\theta) dx_t$$

and the latter integral can be efficiently approximated by drawing N “particles” $x_t^n \sim p(x_t|y_{1:t-1};\cdot)$ then taking the sample average $\sum_{n=1}^N p(y_t|x_t^n;\cdot)/N$, and similarly to approximate $p(y_1|\cdot)$. This can be accomplished using sequential Monte Carlo methods, such as the bootstrap particle filter [[Gordon et al., 1993](#)] given in [Algorithm 1](#). The bootstrap filter returns a non-negative unbiased estimator of the likelihood function $\hat{L}_{PF} \equiv \hat{p}(y_{1:T}|\theta)$, where the expectation of \hat{L}_{PF} is taken with respect to the law underlying the generation of the random variates necessary for the implementation of [Algorithm 1](#). For successful implementations, the number of particles N should be tuned so that the standard deviation of the estimated log-likelihood $\log \hat{L}_{PF}$ does not exceed the value 2 at any given θ , to assure

Algorithm 1 Bootstrap particle filter

Input: Data $y_{1:T}$, number of particles N , and model parameters θ .

Output: The likelihood estimation $\hat{L}_{PF}(\theta)$.

- 1: Initialize particles $\tilde{x}_0^n \sim p(x_0)$.
 - 2: **for** $t = 1, \dots, T$ **do**
 - 3: **if** $t = 1$ **then**
 - 4: For $n = 1, \dots, N$, propagate particles, $x_1^n \sim p(\cdot | \tilde{x}_0^n)$.
 - 5: For $n = 1, \dots, N$, evaluate importance weights, $w_1^n = p(y_1 | x_1^n)$.
 - 6: Estimate $\hat{p}(y_1 | \theta) = \frac{\sum_{n=1}^N w_1^n}{N}$.
 - 7: For $n = 1, \dots, N$, normalize importance weights, $\tilde{w}_1^n = \frac{w_1^n}{\sum_{n=1}^N w_1^n}$.
 - 8: **else**
 - 9: Re-sample N times with replacement from $(x_{t-1}^1, \dots, x_{t-1}^N)$ with associated probabilities $(\tilde{w}_{t-1}^1, \dots, \tilde{w}_{t-1}^N)$ to obtain a new sample $(\tilde{x}_{t-1}^1, \dots, \tilde{x}_{t-1}^N)$.
 - 10: For $n = 1, \dots, N$, propagate particles, $x_t^n \sim p(\cdot | \tilde{x}_{t-1}^n)$.
 - 11: For $n = 1, \dots, N$, evaluate importance weights, $w_t^n = p(y_t | x_t^n)$.
 - 12: Estimate $\hat{p}(y_t | y_{1:t-1}; \theta) = \frac{\sum_{n=1}^N w_t^n}{N}$.
 - 13: For $n = 1, \dots, N$, normalize importance weights, $\tilde{w}_t^n = \frac{w_t^n}{\sum_{n=1}^N w_t^n}$.
 - 14: **end if**
 - 15: **end for**
 - 16: Estimated likelihood $\hat{L}_{PF} := \hat{p}(y | \theta) = \hat{p}(y_1 | \theta) \prod_{t=2}^T \hat{p}(y_t | y_{1:t-1}; \theta)$.
-

good performance of the PMCMC [Pitt et al., 2012], and avoid problems of sticky chains [Sherlock et al., 2015].

The particle Markov chain Monte Carlo algorithm (PMCMC) in Algorithm 2 uses \hat{L}_{PF} in an otherwise standard Metropolis-Hastings algorithm, to sample from the parameter posterior $p(\theta | y_{1:T})$ exactly, for any value of N (Beaumont, 2003, Andrieu and Roberts, 2009), even though N does have an impact on the mixing properties of the algorithm, as discussed below. An algorithm closely related to PMCMC is Monte Carlo within Metropolis (MCWM), given in Algorithm 3 and due to Beaumont [2003] (but see Medina-Aguayo et al., 2016 for theoretical properties). The only difference between MCWM and PMCMC is that in MCWM the likelihood value at the denominator of the acceptance probability is re-estimated anew as $\hat{L}_{PF}(\theta^{r-1})$. That is, at each iteration of MCWM the estimated likelihood at the denominator of α in step 5 of Algorithm 3 is “refreshed”. Notice in particular the double estimations of the likelihood in steps 3–4. Hence, each iteration of the MCWM algorithm requires two estimations of the likelihood function, which is a drawback if the estimation is computationally intensive. The mathematical properties of the MCWM algorithm are less well understood than for PMCMC. The main advantage is, however, that MCWM in many cases generates a chain that mixes better than PMCMC, even when the estimation of the likelihood function is imprecise [Medina-Aguayo et al., 2016]. With MCWM one often avoids problems of stickiness in the simulated Markov chain, a problem that the PMCMC algorithm can suffer from, in particular if the number of particles used in the particle filter is low [Sherlock et al., 2015]. In fact, this causes the estimated likelihoods to have high variability, allowing for the acceptance of the occasional over-estimated $\hat{p}(y_{1:T} | \theta)$ to end-up at the denominator of α in Algorithm 2, hence reducing the chance for newer proposals to be accepted. By “refreshing” the denominator at each iteration, MCWM alleviates this pathology. However, while PMCMC targets the true posterior $p(\theta | y_{1:T})$, this does not hold for MCWM. However, Medina-Aguayo et al. [2016] gives mild conditions on the particle weights such that the stationary distribution targeted by MCWM algorithm will converge to the true posterior distribution as $N \rightarrow \infty$. Simulation results show that, for finite N , the marginal posteriors obtained from MCWM are often wider than the true marginals implied by the PMCMC algorithm, and MCWM therefore generates a conservative estimation of the posterior distribution [Drovandi et al., 2018].

Algorithm 2 PMCMC algorithm

Input: Number of iterations R , starting parameters θ^0 , and corresponding $\hat{L}_{PF}(\theta^0)$.

Output: The chain $\theta^{1:R}$.

```
1: for  $r = 1, \dots, R$  do
2:   Propose  $\theta^* \sim g(\cdot|\theta^{r-1})$ .
3:   Run Algorithm 1 to estimate  $\hat{L}_{PF}(\theta^*)$ .
4:   Compute  $\alpha = \min(1, \frac{\hat{L}_{PF}(\theta^*)}{\hat{L}_{PF}(\theta^{r-1})} \cdot \frac{\pi(\theta^*)}{\pi(\theta^{r-1})} \cdot \frac{g(\theta^{r-1}|\theta^*)}{g(\theta^*|\theta^{r-1})})$ .
5:   Draw  $u \sim \mathcal{U}(0, 1)$ .
6:   if  $u \leq \alpha$  then
7:     Set  $\theta^r = \theta^*$ .
8:   else
9:     Set  $\theta^r = \theta^{r-1}$ .
10:  end if
11: end for
```

Algorithm 3 MCWM algorithm

Input: Number of iterations R , starting parameters θ^0 .

Output: The chain $\theta^{1:R}$.

```
1: for  $r = 1, \dots, R$  do
2:   Propose  $\theta^* \sim g(\cdot|\theta^{r-1})$ .
3:   Run Algorithm 1 to estimate  $\hat{L}_{PF}(\theta^*)$ .
4:   Run Algorithm 1 to estimate  $\hat{L}_{PF}(\theta^{r-1})$ .
5:   Compute  $\alpha = \min(1, \frac{\hat{L}_{PF}(\theta^*)}{\hat{L}_{PF}(\theta^{r-1})} \cdot \frac{\pi(\theta^*)}{\pi(\theta^{r-1})} \cdot \frac{g(\theta^{r-1}|\theta^*)}{g(\theta^*|\theta^{r-1})})$ .
6:   Draw  $u \sim \mathcal{U}(0, 1)$ .
7:   if  $u \leq \alpha$  then
8:     Set  $\theta^r = \theta^*$ .
9:   else
10:    Set  $\theta^r = \theta^{r-1}$ .
11:  end if
12: end for
```

We now introduce in Section 4 elements of Gaussian processes regression, which will be used to construct a surrogate log-likelihood.

4 Modeling the log-likelihood function using Gaussian processes

Gaussian processes (GP) is a class of statistical models that can be used to describe the uncertainty about an unknown function. In our case, the unknown function is the log-likelihood $\ell(\theta) = \log p(y|\theta)$. A GP has the property that the joint distribution for the values of the unknown function, at a finite collection of points, has a multivariate normal distribution. As such each Gaussian process model is fully specified by a mean function m , and a covariance function k [Rasmussen and Williams, 2006]. We introduce a GP regression model as a computationally cheap proxy to the unknown log-likelihood $\ell(\theta)$, the latter being “noisily observed” by means of particle filter approximations $\ell_{PF}(\theta) := \log \hat{L}_{PF}$. The GP regression uses d “covariates”, given by the parameters of interest for our inference problem $\theta = (\theta_1, \dots, \theta_d)$, in addition to several auxiliary parameters later denoted with $\eta = [\phi \ \beta]$. Our GP regression model assumes

$$\ell(\theta) \sim \mathcal{GP}(m_\beta(\theta), k_\phi(\theta, \theta')),$$

where β and ϕ are the auxiliary parameters for the mean and covariance function respectively.

What we want to accomplish with GP regression is to use the parameters proposed during MCWM as covariates, and fit the corresponding log-likelihood values obtained from the particle filter. Once the GP model is fitted to the “training data” produced via MCWM, then for any new θ^* we obtain a proxy to the unknown log-likelihood $\ell(\theta^*)$ that is computationally much faster to evaluate than $\ell_{PF}(\theta^*)$. The training data we fit the GP model to is denoted \mathcal{D} , and how this data is collected is explained in Section 5. Following Drovandi et al. [2018], the unknown log-likelihood function is assumed to be quadratic in θ , and a quadratic mean function m is therefore specified as

$$m_\beta(\theta) = \beta_0 + \sum_{i=1}^d \beta_i \theta_i + \sum_{j \geq i=1}^d \beta_{ij} \theta_i \theta_j = [1 \ \theta_1 \ \theta_2 \ \dots \ \theta_d \theta_d] \beta. \quad (8)$$

In (8) β is a vector of unknown regression coefficients $\beta = [\beta_1, \beta_2, \dots, \beta_{dd}]^\top$. We also assume that the log-likelihood function is a fairly smooth function, and we use an automatic relevance determination squared exponential covariance function (ardSE), defined as

$$k_\phi(\theta, \theta') = \sigma_k \exp(-1/2(\theta - \theta')^\top P^{-1}(\theta - \theta')) + \sigma \mathbf{1}(\theta = \theta'),$$

where P is a diagonal matrix, with diagonal entries $[l_1^2, \dots, l_d^2]$.

The parameters for the covariance function are $\phi = [\sigma \ \sigma_k \ l_1 \ \dots \ l_d]$, where σ is the “nugget”, σ_k the output standard deviation, and the l_i ’s the length scales for each dimension. The full set of parameters for the GP model is therefore $\eta = [\phi \ \beta]$. The mean function is highly parameterized. To avoid over-parameterization it can be useful to use regularization (e.g. using the Lasso, Tibshirani, 1996), if the number of points in the training dataset is small compared to d .

We first pre-estimate β alone using linear regression, to ease the joint optimization problem described in a moment. When pre-estimating β we remove a small number of cases having very low likelihood values. These are considered as outliers and are removed in order to ease the optimization problem. Once this first estimate of β is available, the GP model is fitted to \mathcal{D} using maximum likelihood, i.e. both parameters in $\eta = [\phi \ \beta]$ are jointly estimated (a starting value for β is provided by its pre-estimated value) by minimizing the GP negative log-likelihood $g(\eta)$ with respect to η , where

$$g(\eta) = -\log p(\ell(\theta) | \eta) = (\ell(\theta) - m_\beta(\theta))^\top K_\phi(\Theta, \Theta)^{-1} (\ell(\theta) - m_\beta(\theta)) + \log(\det K_\phi(\Theta, \Theta)) + c. \quad (9)$$

We used $\det(A)$ to denote the determinant of the matrix A , while c is a constant not affecting the optimization. Here Θ denotes the matrix of the θ proposals that belong to the training data \mathcal{D} (see Section 5 for details). The matrix $K_\phi(\Theta, \Theta)$ is the covariance matrix for all the proposals in the matrix Θ . The gradient for the negative log-likelihood (9) is analytically known, and we have that

$$\frac{\partial g}{\partial \beta} = -2m_\beta(\theta)^\top K_\phi(\Theta, \Theta)^{-1}(\ell(\theta) - m_\beta(\theta)\beta),$$

and

$$\begin{aligned} \frac{\partial g}{\partial \phi_i} = & -(\ell(\theta) - m_\beta(\theta)\beta)^\top K_\phi(\Theta, \Theta)^{-1} \frac{\partial K_\phi(\Theta, \Theta)}{\partial \phi_i} K_\phi(\Theta, \Theta)^{-1}(\ell(\theta) - m_\beta(\theta)\beta) + \\ & \text{tr}(K_\phi(\Theta, \Theta)^{-1} \frac{\partial K_\phi(\Theta, \Theta)}{\partial \phi_i}), \end{aligned}$$

where $\text{tr}(A)$ denotes the trace of the matrix A . We can now use a gradient-based optimization algorithm (and in practice we use the conjugate gradient algorithm) to fit the GP model to the training data \mathcal{D} , and we obtain $\hat{\eta} = [\hat{\phi} \quad \hat{\beta}]$ by minimizing (9).

It is simple, and computationally cheap, to generate predictions from the fitted GP model since the predictive distribution is known in closed-form [Rasmussen and Williams, 2006]. This predictive distribution is just the posterior distribution of $\ell(\theta)$ given the training data \mathcal{D} and conditionally to $\hat{\eta}$. That is, for a newly proposed parameter θ^*

$$\ell(\theta^*) | \mathcal{D}, \hat{\eta} \sim \mathcal{N}(\bar{\ell}(\theta^*), \text{Var}(\ell(\theta^*))), \quad (10)$$

where

$$\bar{\ell}(\theta^*) = m_{\hat{\beta}}(\theta^*) + K_{\hat{\phi}}(\theta^*, \Theta) K_{\hat{\phi}}(\Theta, \Theta)^{-1}(\ell(\Theta) - m_{\hat{\beta}}(\Theta)), \quad (11)$$

and

$$\text{Var}(\ell(\theta^*)) = K_{\hat{\phi}}(\theta^*, \theta^*) - K_{\hat{\phi}}(\theta^*, \Theta) K_{\hat{\phi}}(\Theta, \Theta)^{-1} K_{\hat{\phi}}(\Theta, \theta^*). \quad (12)$$

Notice that the (expensive) matrix inversion $K_{\hat{\phi}}(\Theta, \Theta)^{-1}$ in (11)–(12) should only be produced once, since it does not depend on the proposed θ^* .

There are three types of predictions that can be considered:

1. *Mean prediction*: The log-likelihood function at a certain θ^* is deterministically predicted from its mean value at θ^* , that is $\bar{\ell}(\theta^*)$.
2. *Noisy prediction*: Predicting the log-likelihood by sampling from the predictive distribution (10) and including the “nugget” σ in $K_\phi(\theta^*, \theta^*)$. Hence, $K_\phi(\theta^*, \theta^*)$ is computed as $K_\phi(\theta^*, \theta^*) = \sigma_k + \sigma$.
3. *Noise-free prediction*: Sample from (10) where the “nugget” σ is not included, thereby obtaining a non-noisy prediction. The term $K_\phi(\theta^*, \theta^*)$ is therefore computed as $K_\phi(\theta^*, \theta^*) = \sigma_k$.

Same as in Drovandi et al. [2018], we are interested in modeling $\ell(\theta)$, and not a noisy estimate of it, and we will therefore use noise-free predictions. In conclusion, in our delayed-acceptance algorithms we will generate proxies to the unknown $\ell(\theta)$ by sampling from the GP predictive (10) using a noise-free approach.

5 Delayed-acceptance Gaussian process Markov chain Monte Carlo

We now make use of the fitted GP model discussed in Section 4 as a surrogate of the log-likelihood function, to be used in the DA-MCMC and ADA-MCMC algorithms. The likelihood function $L(\theta)$ is assumed intractable and the particle filter estimation $\hat{L}_{PF}(\theta)$ is a non-negative unbiased estimate of it. A cheaper proxy to the true likelihood function at a proposed θ^* can be obtained, after fitting a GP regression model, by sampling the log-likelihood $\ell_{GP}(\theta^*) := \ell(\theta^*)|\mathcal{D}, \hat{\eta}$ from the predictive distribution (10) using a noise-free approach (as defined at the end of Section 4), then denoting with $\hat{L}_{GP}(\theta^*) = \exp(\ell_{GP}(\theta^*))$ the corresponding GP prediction of the likelihood.

Notice that MCMC algorithms based on GP-surrogates have already been considered, e.g. in Meeds and Welling [2014] and Drovandi et al. [2018]. Meeds and Welling [2014] assumes that the latent process has a Gaussian distribution with unknown moments, and these moments are estimated via simulations using the concept of “synthetic likelihood”, as in Wood [2010]. There, the discrepancy between the simulated (Gaussian) latent states and observed data is evaluated using a Gaussian ABC kernel, where ABC stands for “approximate Bayesian computation”, see Marin et al. [2012] for a review. This computationally expensive setting is fitted to “training data”, then used in place of the (unknown) likelihood into a pseudo-marginal MCMC algorithm. The work in Drovandi et al. [2018] builds up on the ideas found in Meeds and Welling [2014], with the difference that the former does not use synthetic likelihoods nor concepts from the ABC approach to produce training data. Instead they use the MCWM algorithm to collect many log-likelihood evaluations at all proposed parameter values, then fit a GP regression model on these training data. Finally, they use the fitted GP regression in a pseudo-marginal algorithm, without ever resorting to expensive likelihood calculations. As opposed to Drovandi et al. [2018], we make use of both a surrogate of the likelihood and (with low frequency) of the expensive likelihood approximated via a particle filter. We call DA-GP-MCMC a delayed acceptance MCMC algorithm using predictions from GP regression as a surrogate of the likelihood function. Similarly, we later introduce our accelerated version ADA-GP-MCMC.

The DA-GP-MCMC procedure is detailed in Algorithm 4 and is preceded by the following two steps, required to collect training data and fit the GP regression to these data (the fitted GP is then used as input to Algorithm 4):

1. *Collect training data using MCWM:* An MCWM algorithm is run as specified in Algorithm 3 (where a particle filter is employed to estimate the likelihood), until the chain has reached apparent stationarity. When using MCWM we do not really target the exact posterior for a finite number of particles N , however, this fact is irrelevant for us. In fact, we use MCWM as in Drovandi et al. [2018], namely to “harvest” a large number of (approximate) likelihood function evaluations. Indeed, in this phase we store as training data \mathcal{D} *all* the proposed parameters θ^* (regardless of whether these are accepted or rejected from the MCWM acceptance criterion) and their corresponding log-likelihoods $\ell_{PF}(\theta^*)$. Hence, all parameter proposals and corresponding log-likelihoods from MCWM (excluding some sufficiently long burn-in period) are stored as training data $\mathcal{D} = \{\theta^{*,i}, \ell_{PF}^{*,i}\}$, (where here the superscript i ranges from 1 to the number of iterations post-burn-in). We also collect the generated Markov chain θ^i and their corresponding log-likelihood estimations θ^i in $\tilde{\mathcal{D}} = \{\theta^i, \ell_{PF}^i\}$. Basically the difference between \mathcal{D} and $\tilde{\mathcal{D}}$ is that parameters θ^i in the latter are the standard output of a Metropolis-Hastings procedure, i.e. $\tilde{\mathcal{D}}$ may contain “repeated parameters” (when rejections occur). Instead \mathcal{D} contains all simulated proposals. The set $\tilde{\mathcal{D}}$ will be used later in Section 5.1.
2. *Fit the GP model:* The Gaussian process model is fitted to the training data \mathcal{D} using the maximum likelihood method described in Section 4.

Using the notation introduced in Section 2, we now have that the first stage acceptance probability for the DA-GP-MCMC algorithm is

$$\alpha_1 = \min\left(1, \frac{\hat{L}_{GP}(\theta^*)}{\hat{L}_{GP}(\theta^{r-1})} \cdot \frac{\pi(\theta^*)}{\pi(\theta^{r-1})} \cdot \frac{g_1(\theta^{r-1}|\theta^*)}{g_1(\theta^*|\theta^{r-1})}\right).$$

The second stage acceptance probability is

$$\alpha_2 = \min\left(1, \frac{\hat{L}_{PF}(\theta^*)}{\hat{L}_{PF}(\theta^{r-1})} \cdot \frac{\hat{L}_{GP}(\theta^{r-1})}{\hat{L}_{GP}(\theta^*)}\right).$$

As mentioned in Section 2, we found it beneficial to use the extended DA-MCMC scheme introduced in Sherlock et al. [2017], where with positive probability β_{MH} it is possible to run a single iteration of a standard PMCMC, with acceptance probability α_{MH} given by

$$\alpha_{MH} = \min\left(1, \frac{\hat{L}_{PF}(\theta^*)}{\hat{L}_{PF}(\theta^{r-1})} \cdot \frac{\pi(\theta^*)}{\pi(\theta^{r-1})} \cdot \frac{g_2(\theta^{r-1}|\theta^*)}{g_2(\theta^*|\theta^{r-1})}\right).$$

When calculating the second acceptance probability α_2 at line 15 in Algorithm 4, it is possible to use a MCWM-style updating scheme, meaning that we recompute $\hat{L}_{PF}(\theta^{r-1})$. Hence, using the MCWM updating scheme for α_2 we have to evaluate the particle filter twice.

Algorithm 4 DA-GP-MCMC algorithm

Input: Number of iterations R , probability to run standard MH update β_{MH} , a GP model fitted to the training data, a starting value θ^0 and corresponding $\hat{L}_{PF}(\theta^0)$ (produced via Algorithm 1).

Output: The chain $\theta^{1:R}$.

```

1: for  $r = 1, \dots, R$  do
2:   Draw  $u \sim \mathcal{U}(0, 1)$ .
3:   if  $u \leq \beta_{MH}$  then ▷ Skip DA-part
4:     Propose  $\theta^* \sim g_2(\cdot|\theta^{r-1})$ .
5:     Run a single iteration of Algorithm 2 for proposal  $\theta^*$ .
6:   else
7:     Propose  $\theta^* \sim g_1(\cdot|\theta^{r-1})$ . ▷ Run two stages DA scheme
8:     Sample from (10) to predict independently  $\ell_{GP}(\theta^*)$  and  $\ell_{GP}(\theta^{r-1})$ . Define  $\hat{L}_{GP}(\theta^*) := \exp(\ell_{GP}(\theta^*))$  and  $\hat{L}_{GP}(\theta^{r-1}) := \exp(\ell_{GP}(\theta^{r-1}))$ .
9:     Compute  $\alpha_1 = \min\left(1, \frac{\hat{L}_{GP}(\theta^*)}{\hat{L}_{GP}(\theta^{r-1})} \cdot \frac{g_1(\theta^{r-1}|\theta^*)}{g_1(\theta^*|\theta^{r-1})} \cdot \frac{\pi(\theta^*)}{\pi(\theta^{r-1})}\right)$ .
10:    Draw  $u \sim \mathcal{U}(0, 1)$ .
11:    if  $u > \alpha_1$  then ▷ Early-reject
12:      Set  $\theta^r = \theta^{r-1}$ .
13:    else
14:      Run Algorithm 1 to estimate the likelihood  $\hat{L}_{PF}(\theta^*)$ . ▷ Second stage update scheme
15:      Compute  $\alpha_2 = \min\left(1, \frac{\hat{L}_{PF}(\theta^*)}{\hat{L}_{PF}(\theta^{r-1})} \cdot \frac{\hat{L}_{GP}(\theta^{r-1})}{\hat{L}_{GP}(\theta^*)}\right)$ .
16:      Draw  $u \sim \mathcal{U}(0, 1)$ .
17:      if  $u \leq \alpha_2$  then ▷ Accept proposal
18:        Set  $\theta^r = \theta^*$ .
19:      else
20:        Set  $\theta^r = \theta^{r-1}$ . ▷ Reject proposal
21:      end if
22:    end if
23:  end if
24: end for

```

5.1 Accelerated delayed-acceptance Gaussian process MCMC

Our accelerated delayed-acceptance Gaussian process MCMC algorithm (ADA-GP-MCMC) is described in Algorithm 5. Same as for DA-GP-MCMC, also ADA-GP-MCMC is preceded by two phases (collection of training data and GP regression). After fitting the GP model, the training data is also used to produce a “selection method” for the four cases introduced in Section 2.1.

As already mentioned in Section 2.1, we can either select which case to use independently of the current proposal θ^* , or make the selection of cases a function of θ^* . We will here introduce three different selection methods, where the first one selects which case to assume independently of θ^* , while the other two depend on the proposal.

- *Biased coin*: The problem of selecting a case between 1 and 3, or between 2 and 4 can be viewed as the result of tossing a biased coin. Hence, for the biased coin model we just compute the relative frequency of occurrence for cases 1, 2, 3 and 4 (see Section 2.1) as observed in the training data. These are obtained as follows: using the fitted GP model we predict log-likelihoods $\ell_{GP}(\theta) \equiv \ell(\theta) | \mathcal{D}, \hat{\eta}$ using (10) for all the collected $\theta \in \Theta$. Then we obtain corresponding $\hat{L}_{GP} := \exp(\ell_{GP}(\theta))$, for all $\theta \in \Theta$. Now, since all the corresponding $\hat{L}_{PF}(\theta)$ are already available as training data, it is possible to compute said relative frequencies \hat{p}_j of occurrence for each case j ($j = 1, \dots, 4$). At iteration r of the ADA-GP-MCMC algorithm, for proposal θ^* and supposing we have passed the first stage then if $\hat{L}_{GP}(\theta^*) > \hat{L}_{GP}(\theta^{r-1})$ we simulate a draw from Bernoulli(\hat{p}_1) and go for case 1 if the draw equals one, and go for case 3 otherwise. If instead $\hat{L}_{GP}(\theta^*) < \hat{L}_{GP}(\theta^{r-1})$ we simulate a draw from Bernoulli(\hat{p}_2) and go for case 2 if the draw equals one, and go for case 4 otherwise.
- *Logistic regression*: The biased coin model above does not take into account the specific value of the current proposal θ^* , that is, the same \hat{p}_j 's are applied to all proposals during a run of ADA-GP-MCMC. We could instead estimate $\hat{p}_j(\theta)$ using logistic regression. In this setting we have two logistic regression models to estimate, one for cases 1 and 3, and one for cases 2 and 4. These models are estimated on the training data \mathcal{D} . By combining the training data \mathcal{D} , and the accepted proposals stored in $\tilde{\mathcal{D}}$ we then have access to both the particle filter evaluations for all proposals, and for the accepted proposals. Using \mathcal{D} and $\tilde{\mathcal{D}}$ we can now classify which case each proposal *should* belong to. This is done by computing GP predictions, independently for both sets of parameters stored in \mathcal{D} and $\tilde{\mathcal{D}}$. Note, after computing the GP predictions we have (i) particle filter predictions and GP predictions for all proposals in \mathcal{D} , i.e. $\hat{L}_{PF}(\theta^*)$ and $\hat{L}_{GP}(\theta^*)$, and (ii) particle filter predictions and GP predictions for all accepted proposals in $\tilde{\mathcal{D}}$, hence, $\hat{L}_{PF}(\theta^{r-1})$ and $\hat{L}_{GP}(\theta^{r-1})$. We can now loop over the proposals in the training data and assign labels for which of the four cases each proposal belongs to. As an example, after labelling is performed, all proposals in the training data that are classified to belong to case 1 or 3 are denoted $\theta_{1,3}^*$, and an associated indicator vector $y_{1,3}$ having 1's for proposals belonging to case 1 and 0's for proposals belonging to case 3. We can now fit a logistic regression model on $\{\theta_{1,3}^*, y_{1,3}\}$, where the $\theta_{1,3}^*$ take the role of "covariates" and $y_{1,3}$ are binary "responses". We denote with $\hat{p}_1(\theta)$ the resulting fitted probability of selecting case 1 (so that $\hat{p}_3(\theta) = 1 - \hat{p}_1(\theta)$). In a similar way, after labelling is performed, all proposals in the training data that are classified to belong to case 2 or 4 are denoted $\theta_{2,4}^*$, with associated indicator vector $y_{2,4}$. We fit a logistic regression model on $\{\theta_{2,4}^*, y_{2,4}\}$ to obtain $\hat{p}_2(\theta)$ (and $\hat{p}_4(\theta) = 1 - \hat{p}_2(\theta)$).

All the above is preliminary to starting ADA-GP-MCMC. Then we proceed as described for the biased coin case, with minimal notation adjustment. Namely for a new proposal θ^* , if $\hat{L}_{GP}(\theta^*) > \hat{L}_{GP}(\theta^{r-1})$ we decide between case 1 and 3 by drawing from Bernoulli($\hat{p}_1(\theta^*)$). If instead $\hat{L}_{GP}(\theta^*) < \hat{L}_{GP}(\theta^{r-1})$ we simulate from Bernoulli($\hat{p}_2(\theta^*)$) to decide between case 2 and 4.

- *Decision tree*: The decision tree model employs the same idea as the logistic regression model. Decision trees can be better at modeling non-linear dependencies in the data. Importantly, the decision tree model does not produce an estimation of the probabilities for each case (hence, we do not obtain a direct estimation of $\hat{p}_j(\theta)$), instead a classification decision is computed. However, the classification decision can directly be used to select which case to assume. Now, assuming that we are at iteration r of ADA-GP-MCMC and that we have to select between cases 1 and 3, the decision tree model will now directly tell us which case to select, for the given proposal θ^* .

Our experience shows that the decision tree model is the preferred method to use, since this seems to perform best at capturing the complex non-linear relationships in the training data. We have found beneficial to include, as a covariate in the decision tree model, the ratio between the GP-based log-likelihood estimate at the current proposal and corresponding old log-likelihood estimate.

In conclusion, we have introduced three selection methods, that use different approaches to determine which case a proposal should be passed to. In Algorithm 5 the selection methods are denoted $s_{13}()$ (for selection between case 1 and 3) and $s_{24}()$ (for selecting between case 2 and 4), to highlight the fact that different selection methods are available. In Appendix A we describe how to test the fit of the GP model and the performance of the selection method.

Algorithm 5 ADA-GP-MCMC algorithm

Input: Number of iterations R , probability to run standard MH update β_{MH} , a GP model fitted to the training data, model $s_{13}()$ to select between case 1 and 3, model $s_{24}()$ to select between case 2 and 4, a starting value θ^0 and corresponding L^0 (the latter produced via Algorithm 1).

```

1: for  $r = 1, \dots, R$  do
2:   Draw  $u \sim \mathcal{U}(0, 1)$ .
3:   if  $u \leq \beta_{MH}$  then ▷ Skip DA-part
4:     Propose  $\theta^* \sim g_2(\cdot|\theta^{r-1})$ .
5:     Run Algorithm 2 for one iteration using the proposal  $\theta^*$ .
6:   else
7:     Propose  $\theta^* \sim g_1(\cdot|\theta^{r-1})$ . ▷ Run A-DA scheme
8:     Sample from the predictive distribution of the GP model to predict independently  $\ell_{GP}(\theta^*)$ 
      and  $\ell_{GP}(\theta^{r-1})$ . Define  $\hat{L}_{GP}(\theta^*) := \exp(\ell_{GP}(\theta^*))$  and  $\hat{L}_{GP}(\theta^{r-1}) := \exp(\ell_{GP}(\theta^{r-1}))$ .
9:     Compute  $\alpha_1 = \min\left(1, \frac{\hat{L}_{GP}(\theta^*)}{\hat{L}_{GP}(\theta^{r-1})} \cdot \frac{g_1(\theta^{r-1}|\theta^*)}{g_1(\theta^*|\theta^{r-1})} \cdot \frac{\pi(\theta^*)}{\pi(\theta^{r-1})}\right)$ .
10:    Draw  $u \sim \mathcal{U}(0, 1)$ .
11:    if  $u < \alpha_1$  then ▷ Run second stage of the A-DA scheme
12:      if  $\hat{L}_{GP}(\theta^*) > \hat{L}_{GP}(\theta^{r-1})$  then
13:        Select case 1 or 3 according to the model  $s_{13}(\theta^*)$ .
14:        Run the accelerated delayed-acceptance scheme for the selected case.
15:      else
16:        Select case 2 or 4 according to the model  $s_{24}(\theta^*)$ .
17:        Run the accelerated delayed-acceptance scheme for the selected case.
18:      end if
19:    else ▷ Early-reject
20:      Set  $\theta^r = \theta^{r-1}$ .
21:    end if
22:  end if
23: end for

```

6 Implementation details

Unless else stated, all calculations were carried out on the LUNARC cluster available at Lund University (Sweden), where each node has access to two Intel Xeon E5-2650 v3 (2.3 Ghz, 10-core) CPUs, <http://www.lunarc.lu.se>. The algorithms are implemented with Julia 0.5.2 [Bezanson et al., 2017], and the code is available at <https://github.com/SamuelWiqvist/adamcmcpaper>.

For the considered case studies, the parameters in θ are all positive, and for convenience we conduct inference on their natural logarithms. The prior distributions will also be set on the log-scale. The weights w_t^n in the particle filter can sometimes take very large and small values, and for numerical stability these are computed on the log-scale. We also make use of standard methods such as subtracting the largest log-weight at time t from the log-weights at time t , prior to exponentiate them

[Cappé et al., 2007]. Regarding the computation of the sum of the weights, required to compute the denominator of the normalized weights \tilde{w}_t^n , the so-called log-sum-exp trick turns useful [Murphy, 2012]. In Algorithm 1 particles are resampled using the stratified resampling algorithm [Kitagawa, 1996]. The execution of the bootstrap filter for the Ricker model (Section 7.1) is relatively cheap, since the model is fairly simple and the data set used is small (it only contains $T = 50$ observations). We can, therefore, easily compute exact Bayesian inference by using the PMCMC algorithm, since it is possible to run the particle filter with sufficiently many particles, so that the standard deviation of the estimated log-likelihood is less than 2, thereby obtaining an algorithm with good performance [Pitt et al., 2012], and avoid problems of sticky chains [Sherlock et al., 2015].

The DWP-SDE model in Section 7.2 is a more complex case study, and the particle filter is time-consuming since the data set contains 25,000 observations. On a standard desktop computer it can therefore be computational unfeasible to run the PMCMC algorithm. We will assign $N \approx 200 - 500$ particles to separate cores of the LUNARC cluster (possibly over multiple nodes), and run independent particle filters in parallel (this can also be replicated on a multiprocessor desktop by running several independent estimations of the likelihood). A simple method, exploiting multiple particle filters running in parallel on multiple cores (or multiple CPUs), is in Drovandi [2014], and consists of averaging out likelihood approximations obtained at different cores. Since the likelihood approximations are computed on the log-scale we have to compute the average of the exponential of the log-likelihood approximation, and then take the logarithm of this average. This scheme allows us to obtain an unbiased approximation of the likelihood function with lower variance, compared to the approximation obtained from a single particle filter. The negative log-likelihood function g in (9) is minimized using the function `optimize`, found in the Julia package `Optim.jl`. In particular, we used a conjugate-gradient algorithm. As a measure of efficiency of the different Markov chains produced by the different algorithms, we compute the minimal ESS/(time unit), where ESS is the effective sample size. That is, the ESS for each parameter’s chain is obtained via the R-package `mcmcse`, then the minimum ESS value across all chains is found, and this value is then divided by the run-time. Hence, `min ESS/(time unit)` tells us how many independent samples the algorithm is generating per time-unit, when we consider the least efficient chain.

7 Case studies

We now use PMCMC, MCWM, DA-GP-MCMC, and ADA-GP-MCMC algorithms to perform Bayesian inference for the parameters of two dynamical models with intractable likelihood functions. We emphasize that the most important comparison between methods is the one that considers results from DA-GP-MCMC and ADA-GP-MCMC. In fact, the latter aims at improving the computational performance of DA-GP-MCMC, while being an approximate (and accelerated) delayed acceptance algorithm. Hence, the inference results returned by ADA-GP-MCMC should be directly compared with DA-GP-MCMC, while the other two methods provide further (but less relevant) comparisons.

In Section 7.1 we consider the Ricker model, which has been used numerous times as toy model to compare inference methods (e.g. Fearnhead and Prangle [2012], Fasiolo et al. [2016] to name a few). In Section 7.2 we consider a novel double-well potential stochastic differential equation model for protein folding data, which is a considerably more complex case study. Further results, including residual plots for the GP model, are presented in the supplementary material.

7.1 Ricker Model

The Ricker model is used in ecology to describe how the size of a population varies in time and follows

$$\begin{cases} y_{t+1} \sim \mathcal{P}(\phi x_{t+1}), \\ x_{t+1} = r x_t e^{-x_t + \epsilon_t}, \epsilon_t \stackrel{iid}{\sim} \mathcal{N}(0, \sigma), \end{cases} \quad (13)$$

where $\mathcal{P}(\lambda)$ is the Poisson distribution with mean λ . The $\{x_t\}$ process is a latent (i.e. unobservable) Markov process and realizations from the observable process $\{y_t\}$ are conditionally independent given the latent states, since the ϵ_t are assumed independent. Even though the model is fairly simple its dynamics are highly non-linear and close to chaotic for some choice of the parameter values [Wood, 2010]. The likelihood function is also both analytically and numerically intractable, if evaluated at parameters very incompatible with the observed data, see Fasiolo et al. [2016] for a review of inference methods applied to the Ricker model.

The unknown parameters we are interested in estimating are $\theta = [\log r, \log \phi, \log \sigma]$, and we use PMCMC, MCWM, DA-GP-MCMC, and ADA-GP-MCMC for this task. That is, MCWM is not only used to provide the training data for fitting a GP regression, but also to provide inference results, in the interest of comparison between methods. PMCMC is used to provide exact Bayesian inference. A data set containing $T = 50$ observations, generated from the model with ground-truth parameters $\theta_{true} = [3.80, 2.30, -1.20]$ at integer sampling times $t \in [1, 2, \dots, T]$, is presented in Figure 1, and the starting value x_0 for the latent state was deterministically set to $x_0 = 7$ and considered as a known constant throughout.

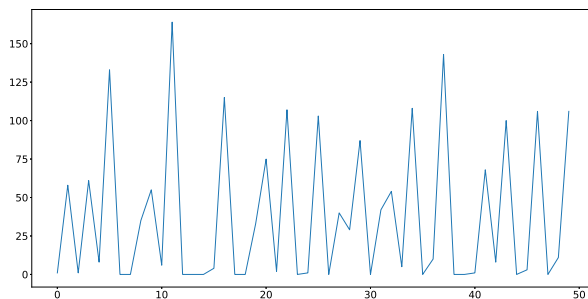


Figure 1: Data generated from the Ricker model.

Results obtained with PMCMC and MCWM are produced using in total 52,000 iterations (including a burn-in period of 2,000 iterations), and $N = 1,000$ particles (the standard deviation of the log-likelihood obtained from the particle filter is about 0.5). The proposal distribution was adaptively tuned using the generalized AM algorithm (Andrieu and Thoms, 2008, Mueller, 2010), which is set to target an acceptance rate of 40%.

For DA-GP-MCMC algorithm, we used the last 2,000 iterations of a previous MCWM run to obtain training data. Prior to fitting the GP model we removed the 10% of the cases having the lowest log-likelihood values from the the training data. After fitting the GP model, we set $\beta_{MH} = 0.15$ (that is a 15% probability to skip the delayed-acceptance step and execute a regular Metropolis-Hastings step), $N = 1,000$, and ran DA-GP-MCMC for further 50,000 iterations. The Gaussian kernels for the Metropolis random walks, g_1 and g_2 , were kept fixed during the entire run of the DA-GP-MCMC algorithm: specifically, g_2 used the covariance matrix Σ returned by the final iteration of the MCWM algorithm that was used to collect training data, and g_1 was set to a kernel having slightly larger terms in the covariance, i.e. we used a covariance $a^2\Sigma$ with $a > 1$. An important modification of DA-GP-MCMC as described in Algorithm 4, is that in our case studies the value $\hat{L}_{PF}(\theta^{r-1})$ at the denominator of α_2 is “refreshed”. Hence, we employ a MCWM updating procedure in the second stage. This is to obtain a reasonable high acceptance rate and to avoid problems with stickiness. The same modification was used for ADA-GP-MCMC. At the second-stage of the r -th iteration of ADA-GP-MCMC, a decision tree model was used to select a case from the four ones discussed in sections 2.1 and 5.1, based on the values of the variables $\left[\theta^*, \frac{\hat{L}_{GP}(\theta^*)}{\hat{L}_{GP}(\theta^{r-1})} \right]$.

Wide uniform priors were employed for all unknown parameters; $\pi(\log r) \sim \mathcal{U}(0, 10)$, $\pi(\log \phi) \sim \mathcal{U}(0, 4)$ and $\pi(\log \sigma) \sim \mathcal{U}(-10, 1)$. The starting values were also deliberately set far away from the

true parameter values: $\log r_0 = 1.10$, $\log \phi_0 = 1.10$, and $\log \sigma_0 = 2.30$. Results are presented in Table 1 and Figure 2. We can conclude that all parameters are well inferred. The results for the different algorithms are also similar. The parameter with the highest estimation uncertainty is σ , which is in not surprising since σ is the parameter that governs the noise in the model, and this is often the hardest parameter to estimate from discretely observed measurements. Notice that results produced by ADA-GP-MCMC are essentially identical to those from DA-GP-MCMC, which is very encouraging as from the remark at the beginning of Section 7. That is the most relevant way to judge inference results from the accelerated ADA procedure is to compare those to the standard DA algorithm rather than, say, PMCMC.

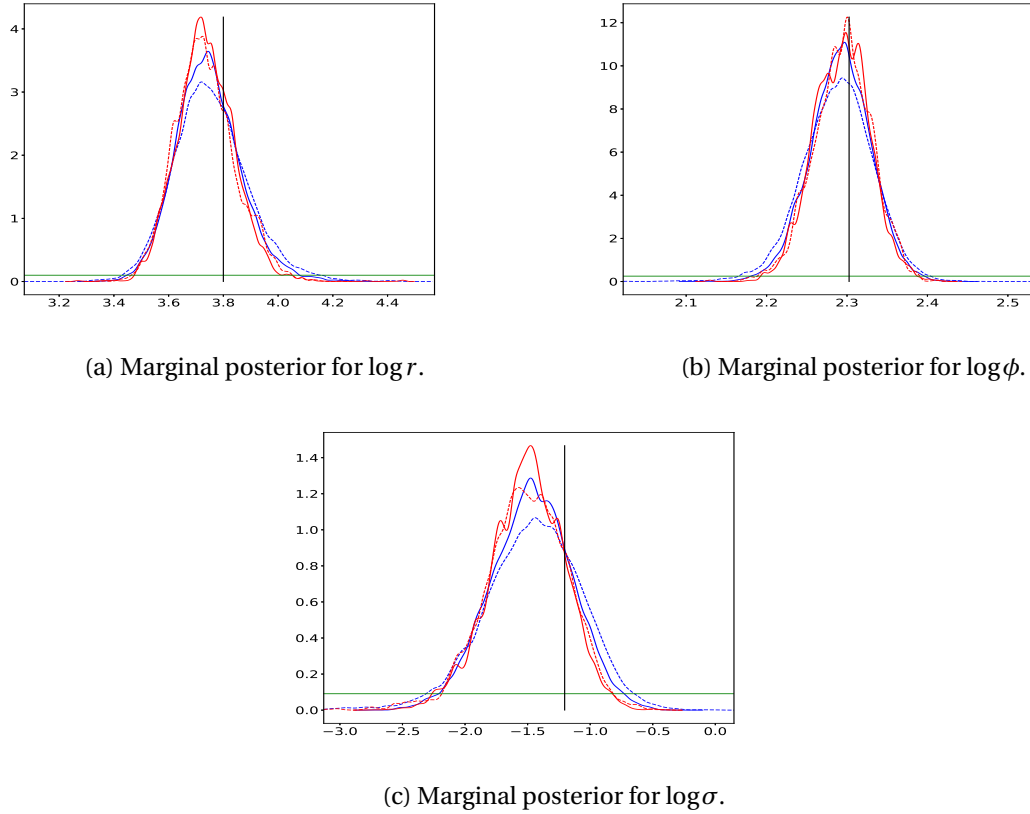


Figure 2: Marginal posteriors: PMCMC (blue solid line), MCWM (blue dashed line), DA-GP-MCMC (red solid line), and ADA-GP-MCMC (red dashed line). Priors distributions are denoted with green lines (these look “cut” as we zoom on the bulk of the posterior), and the true parameter values are marked with black vertical lines.

Table 1: Posterior means (2.5th and 97.5th quantiles) for PMCMC, MCWM, DA-GP-MCMC, and ADA-GP-MCMC.

	True value	PMCMC	MCWM	DA-GP-MCMC	ADA-GP-MCMC
$\log r$	3.80	3.75 [3.53, 4.00]	3.75 [3.51, 4.05]	3.74 [3.54, 3.96]	3.73 [3.54, 3.97]
$\log \phi$	2.30	2.29 [2.21, 2.36]	2.29 [2.20, 2.37]	2.29 [2.23, 2.36]	2.29 [2.22, 2.36]
$\log \sigma$	-1.58	-1.47 [-2.13, -0.85]	-1.46 [-2.3, -0.75]	-1.5 [-2.12, -0.95]	-1.51 [-2.16, -0.92]

Properties of the algorithms are presented in Table 2. Before discussing these results, we emphasize that the benefits of our accelerated procedure are to be considered when the case study has a like-

Table 2: Algorithm properties for the the PMCMC, MCWM, DA-GP-MCMC, and ADA-GP-MCMC algorithm.

	Seconds per 1000 iter.	Acceptance rate (%)	min ESS/sec	Skip DA run MH update (%)	Early- rejections (%)
PMCMC	20.26	40.21	2.53	NA	NA
MCWM	39.83	39.70	1.26	NA	NA
DA-GP-MCMC	10.32	7.66	1.99	14.75	81.05
ADA-GP-MCMC	9.46	7.89	1.75	15.02	80.49

Table 3: Estimated probabilities for the different cases and percentage of times the assumption for the different cases in the ADA-GP-MCMC algorithm holds.

	Case 1	Case 2	Case 3	Case 4
Est. probab. ($\hat{p}_1, \hat{p}_2, \hat{p}_3, \hat{p}_4$)	0.59	0.91	0.41	0.09
Perc. assum. holds	73.51	88.24	39.80	21.21

likelihood that is computationally very challenging, and this is not the case for the present example, see instead Section 7.2. The ADA-GP-MCMC algorithm is the fastest algorithm, though only marginally faster than DA-GP-MCMC (4.2 times faster than MCWM and 1.09 times faster than DA-GP-MCMC), while MCWM is the slowest one. Not surprisingly, PMCMC is almost twice as fast as MCWM, and this is because PMCMC only requires one evaluation of the particle filter per iteration, while the MCWM requires two evaluations. The four algorithms are, however, essentially equally efficient, as from the min ESS/sec values.

The estimated probabilities \hat{p}_j for the four different cases characterizing ADA-GP-MCMC (recall that $\hat{p}_3 = 1 - \hat{p}_1$ and $\hat{p}_4 = 1 - \hat{p}_2$), and the percentage for each case to hold, i.e. the probability that the selected case indeed is the correct one, are presented in Table 3 (computed using the method described in Appendix A). We notice that the probability for the different cases vary considerably, and also that the percentages that the assumption holds vary for the different cases.

7.2 Double-well potential stochastic differential equation model for protein folding data

We now consider a computationally intensive case study concerning statistical inference for protein folding data. The challenges for this case study are: (a) the sample size is large, data being a long time-series (about 2.5×10^4 observations); (b) the non-linear dynamics, and (c) the presence of local perturbations. ‘‘Protein folding’’ is the last and crucial step in the transformation of genetic information, encoded in DNA, into functional protein molecule. Studying the time-dynamics of real protein folding dynamics results in a very high dimensional problem, which is difficult to analyze using exact Bayesian methodology. Therefore, for reasons of simplification and tractability, the dynamics of a protein are often modelled as diffusions along a single ‘‘reaction coordinate’’, that is one-dimensional diffusion models are considered to model a projection of the actual dynamics in high-dimensional space (Das et al., 2006, and references therein).

We consider two protein folding (reaction coordinate) data sets, presented in Figure 3 and 4. In these figures we see that data have a marginal bimodal structure, with irregular change-points where the mean of the data shifts, and a local noisy structure. A class of models shown to be suitable for statistical modeling of protein folding (at least when these data result into a low-dimensional projection of the original data) is given by stochastic differential equations (SDEs), see Forman and Sørensen [2014] and Picchini and Forman [2016]. Monte Carlo inference methods are very computationally intensive for these models (in Picchini and Forman, 2016 sub-sampling methods and approximate Bayesian computation methods were used to accelerate the inference problem). We now introduce

a novel double-well potential stochastic differential equation (DWP-SDE) model for protein folding data. This model is faster to simulate than the one proposed in [Forman and Sørensen \[2014\]](#) and [Picchini and Forman \[2016\]](#).

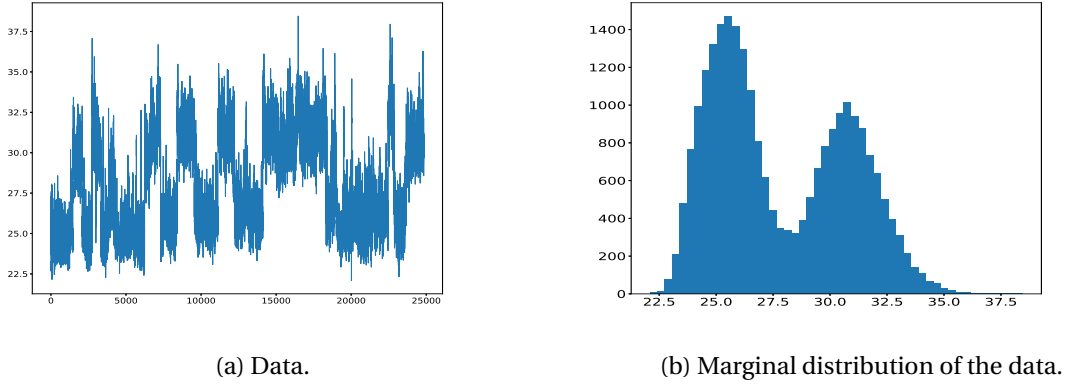


Figure 3: Data set 1.

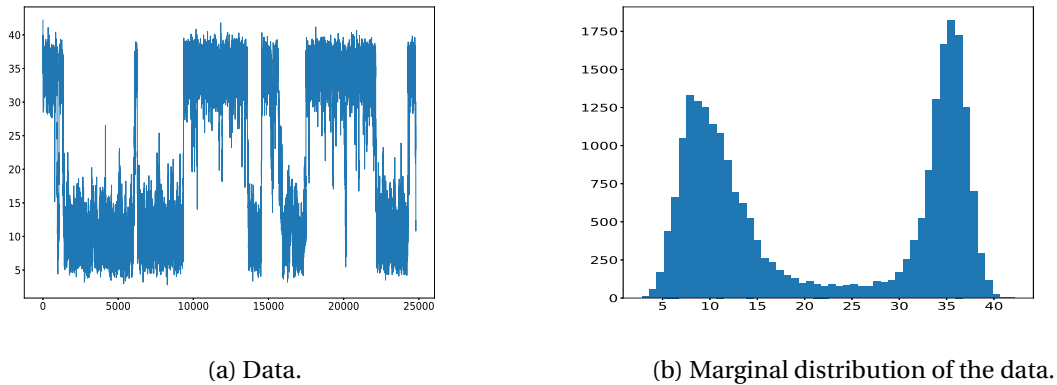


Figure 4: Data set 2.

Our DWP-SDE model is defined as

$$\begin{cases} z_t = x_t + y_t, \\ dx_t = -\nabla V(x_t) dt + \sigma dW_t^x, \\ dy_t = -\kappa y_t dt + \sqrt{2\kappa\gamma^2} dW_t^y. \end{cases} \quad (14)$$

Here $\{z_t\}$ is the observable process, consisting in the sum of the solutions to the double-well potential SDE process $\{x_t\}$ and process $\{y_t\}$, the latter being unobservable and representing autocorrelated error. Here $\nabla V(\cdot)$ is the gradient of the double-well potential function $V(\cdot)$ with respect to x_t . Finally W_t^X and W_t^Y are independent standard Wiener processes, that is their increments dW_t^X and dW_t^Y are independent, Gaussian distributed with zero mean and variance dt .

We consider the following double-well potential function

$$V(x, c, d, A, g, p_1, p_2) = \frac{1}{2} \left| \frac{1}{2} |x - c|^{p_1} - d + gx \right|^{p_2} + \frac{1}{2} Ax^2, \quad (15)$$

which is based on the potential described in equation 1 in [Fang et al. \[2017\]](#). The formulation in (15) is fairly general, in the sense that many different potentials can be specified by varying its parameters. The parameters in (15) have the following interpretation: c specifies the location for the

potential (i.e. where the potential is centered); d determines the spread of the potential; A is an asymmetry parameter; g compresses the two modes of the long term (stationary) density of process $\{X_t\}$; parameters p_1 and p_2 control the shape of the two modes (if the parameters p_1 and p_2 are set to low values the long term probability distribution becomes more flat with less distinct modes); σ governs the noise in the latent $\{X_t\}$ process. The error-model Y_t is an Ornstein-Uhlenbeck process specified by two parameters: κ is the autocorrelation level, and γ is the noise intensity. In principle, inference should be conducted for $[\log \kappa, \log \gamma, \log A, \log c, \log d, \log g, \log p_1, \log p_2, \log \sigma]$. However, the model parameters A and g are “stiff”, i.e. small changes in their values result in considerable changes in the output, and are therefore hard to estimate. Estimating all the parameters of the DWP-SDE model is also a complex task since a larger data set seems needed to capture the stationary distribution of the data. We will therefore consider the easier task of estimating the parameters $\theta = [\log \kappa, \log \gamma, \log c, \log d, \log p_1, \log p_2, \log \sigma]$. The remaining parameters, A and g , will be fixed to arbitrary values, as discussed later.

Simulating the y_t process in (14) is easy since the transition density for the Ornstein-Uhlenbeck process is known. We have that

$$y_t | y_s = x \sim \mathcal{N}(x e^{-\kappa \Delta_t}, \gamma^2 (1 - e^{-2\kappa \Delta_t})),$$

where $\Delta_t = t - s$, for $s < t$. The transition density for the x_t process is not analytically known, and we use the Euler-Maruyama scheme to propagate the x_t process, that is we use

$$x_{t+\delta_t} | x_t = x \approx x - \nabla V(x) \delta_t + \sigma \epsilon_t,$$

where $\epsilon_t \sim \mathcal{N}(0, \delta_t)$, and $\delta_t > 0$ is the stepsize for the Euler-Maruyama numerical integration scheme (typically $\delta_t \ll \Delta_t$).

Let us now consider the likelihood function for the z_t process in (14), for a set of discrete observations $\mathbf{z} = [z_1, \dots, z_T]$ that we assume observed at integer sampling times $t \in [1, 2, \dots, T]$. Corresponding (unobservable) values for the X_t process at the same sampling times are $[x_1, \dots, x_T]$. In addition, we denote with \mathbf{x} the set $\mathbf{x} = [x_0, x_1, \dots, x_T]$, which includes an arbitrary value x_0 from which simulations of the latent system are started. The likelihood function can be written as

$$\begin{aligned} L(\theta) &= p(\mathbf{z} | \theta) = p(z_1 | \theta) \prod_{t=2}^T p(z_t | z_1, \dots, z_{t-1}, \theta) \\ &= \int p(z_1, \dots, z_T | x_0, \dots, x_T, \theta) p(x_0, \dots, x_T | \theta) dx_0 \cdots x_T \\ &= \int p(z_1, \dots, z_T | x_0, \dots, x_T, \theta) p(x_0) \prod_{t=1}^T p(x_t | x_{t-1}, \theta) dx_0 \cdots x_T. \end{aligned}$$

The last product in the integrand is due to the Markov property of X_t . Also, we have introduced a density $p(x_0)$, and if x_0 is deterministically fixed (as in our experiments) this density can be discarded. We cannot compute the likelihood function analytically (as the integral is typically intractable), but we can use sequential Monte Carlo (for example, the bootstrap filter in Algorithm 1) to compute an unbiased approximation $\hat{p}(\mathbf{z} | \theta)$, which allows us to use PMCMC or MCWM for the inference. Furthermore, the Z_t process is a transformation of the measurement noise that follows an Ornstein-Uhlenbeck process, and the density for $p(z_1, \dots, z_T | x_0, \dots, x_T, \theta)$ is known [Picchini and Forman, 2016]. We have that

$$p(z_1, \dots, z_T | x_0, \dots, x_T, \theta) = \frac{1}{\gamma} \cdot \phi\left(\frac{z_1 - x_1}{\gamma}\right) \cdot \prod_{t=2}^T \frac{1}{\gamma \sqrt{1 - e^{-2\kappa \Delta_t}}} \cdot \phi\left(\frac{z_t - x_t - e^{-\kappa \Delta_t} (z_{t-1} - x_{t-1})}{\gamma \sqrt{1 - e^{-2\kappa \Delta_t}}}\right),$$

where $\Delta_t = t_i - t_{i-1}$, and $\phi(\cdot)$ denotes the density function for the standard Gaussian distribution.

We now explain how an unbiased approximation to $p(\mathbf{z} | \theta)$ is computed. To facilitate this explanation we introduce following notation: let $x_{t-1}^{1:N}$ denote the set of N particles we have at time $t - 1$

before resampling is performed (see Algorithm 1 for reference on the terminology). Let $\tilde{x}_{t-1}^{1:N}$ denote the resampled particles that are used to propagate the latent system forward to time t (using Euler-Maruyama). We approximate $p(z|\theta)$ with $\hat{p}(z|\theta)$ as

$$\hat{p}(z|\theta) = \hat{p}(z_1|\theta) \prod_{t=2}^T \hat{p}(z_t|z_1, \dots, z_{t-1}, \theta) = \hat{p}(z_1|\theta) \left\{ \prod_{t=2}^T \frac{1}{N} \sum_{n=1}^N w_t^n \right\},$$

where the weights w_t^n are

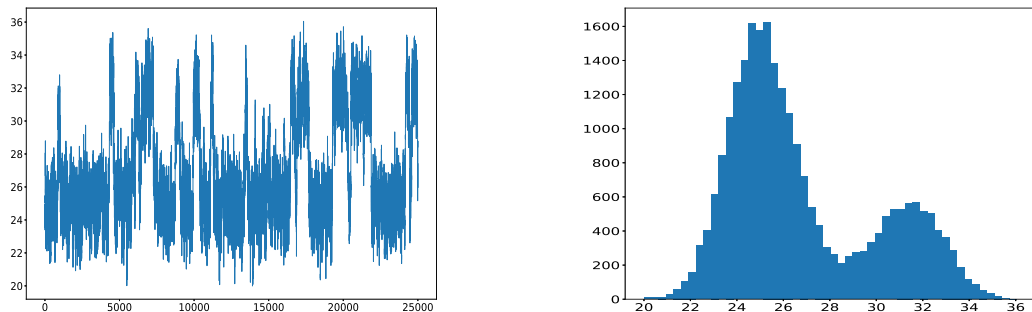
$$w_t^n = \frac{1}{\gamma \sqrt{1 - e^{-2\kappa\Delta_t}}} \cdot \phi\left(\frac{z_t - x_t^n - e^{-\kappa\Delta_t}(z_{t-1} - \tilde{x}_{t-1}^n)}{\gamma \sqrt{1 - e^{-2\kappa\Delta_t}}}\right), \quad t \geq 2$$

and

$$\hat{p}(z_1|\theta) = \frac{1}{N} \sum_{n=1}^N w_1^n, \quad \text{with } w_1^n = \frac{1}{\gamma} \cdot \phi\left(\frac{z_1 - \tilde{x}_1^n}{\gamma}\right).$$

7.2.1 Simulation study

Here we simulate data from model (14), and then produce Bayesian inference for the parameters. Simulated data of length $T = 25,000$ are produced using ground-truth parameters θ_{true} set to $\exp(\theta_{\text{true}}) = [0.3, 0.9, 0.01, 28.5, 4, 0.03, 1.5, 1.8, 1.9]$. The simulated data are reported in Figure 5. The parameters were set to produce data resembling data set 1 in Figure 3.



(a) Simulated data.

(b) Marginal distribution of the simulated data.

Figure 5: Data generated from the DWP-SDE model.

We set Gaussian priors on the parameters: $\pi(\log \kappa) \sim \mathcal{N}(-0.7, 0.5^2)$, $\pi(\log \gamma) \sim \mathcal{N}(-0.7, 0.5^2)$, $\pi(\log c) \sim \mathcal{N}(3.34, 0.173^2)$, $\pi(\log d) \sim \mathcal{N}(1.15, 0.2^2)$, $\pi(\log p_1) \sim \mathcal{N}(0.69, 0.5^2)$, $\pi(\log p_2) \sim \mathcal{N}(0, 0.5^2)$, and $\pi(\log \sigma) \sim \mathcal{N}(0, 0.5^2)$. The starting parameter values were set far from the ground truth, as $\exp(\theta_0) = [2, 2, 30, 10, 2, 2, 2]$.

For each iteration of MCWM we compute 4 unbiased approximations of the likelihood function, one for each core of our computer, using $N = 200$ particles for each of the 4 likelihoods. Taking the sample average of these likelihoods produces another unbiased estimate of the likelihood, but with a smaller variance than the individual ones (this is theoretically true and also studied in detail in Drovandi, 2014). However, given the length of the time-series, the obtained approximated likelihood is still fairly variable, and should we use PMCMC this would produce sticky chains. Therefore MCWM comes to our help for this example, as “refreshing” the denominator of the acceptance ratio helps escaping from sticky points, occurring when the likelihood approximation is overestimated.

We used the following settings with MCWM: 20,000 iterations; burn-in of 10,000 iterations; the proposal distribution was adaptively tuned, by using the generalized AM algorithm (Andrieu and

Table 4: Parameter estimations (posterior mean and posterior quantile interval (2.5th and 97.5th quantile)) for MCWM, DA-GP-MCMC, and ADA-GP-MCMC.

	True value	MCWM	DA-GP-MCMC	ADA-GP-MCMC
$\log \kappa$	-1.2	-1.2 [-1.43,-0.97]	-1.21 [-1.43,-0.99]	-1.21 [-1.44,-0.95]
$\log \gamma$	-0.11	-0.11 [-0.25,0.02]	-0.1 [-0.24,0.01]	-0.11 [-0.25,0.03]
$\log c$	3.35	3.35 [3.34,3.36]	3.35 [3.34,3.36]	3.35 [3.34,3.36]
$\log d$	1.39	1.44 [1.17,1.81]	1.41 [1.18,1.69]	1.43 [1.16,1.85]
$\log p_1$	0.41	0.43 [0.29,0.63]	0.42 [0.29,0.57]	0.43 [0.28,0.65]
$\log p_2$	0.59	0.51 [0.1, 0.82]	0.54 [0.18,0.88]	0.52 [0.02,0.92]
$\log \sigma$	0.64	0.65 [0.48,0.81]	0.64 [0.49,0.77]	0.65 [0.48,0.79]

Table 5: Algorithm properties for the the MCWM, DA-GP-MCMC, and ADA-GP-MCMC algorithm.

	Minutes per 1000 iter.	Acceptance rate (%)	min ESS/min	Second stage direct (%)	Early-rejections (%)
MCWM	60.29	19.84	0.57	NA	NA
DA-GP-MCMC	20.67	3.80	0.67	15.01	67.03
ADA-GP-MCMC	13.39	4.02	1.04	15.10	67.01

Thoms, 2008, Mueller, 2010), set to target an acceptance rate of 15%. The training part for DA-GP-MCMC and ADA-GP-MCMC was the output of an MCWM algorithm with the settings specified above. We fit a GP model to the output from the first 5,000 iterations of MCWM obtained after burn-in (we only removed 1% of the observations in the training data with the lowest log-likelihood values from the training data, prior to fitting the GP model). In a similar manner as for the Ricker model the two transition kernels g_1 and g_2 were based on the covariance matrices returned by the final iteration of the MCWM algorithm. A decision tree model, similar to the one used for the Ricker model, was used for the selection problem. Then we ran DA-GP-MCMC and ADA-GP-MCMC for 10,000 iterations, using $\beta_{MH} = 0.15$. Same as with the Ricker model, an MCWM-style updating scheme was used in the second stage of both DA and ADA algorithms.

Table 6: Estimated probabilities for the different cases and percentage of times the assumption for the different cases in the ADA-GP-MCMC algorithm holds.

	Case 1	Case 2	Case 3	Case 4
Est. prob. $(\hat{p}_1, \hat{p}_2, \hat{p}_3, \hat{p}_4)$	0.22	0.90	0.78	0.09
Perc. assum. holds	38.05	84.40	69.17	27.90

Marginal posteriors from the two methods are in Figure 6. These results very similar, given the diffuse priors (also, see the posterior quantile intervals in Table 4). From Table 5 we see that the speed-up for ADA-GP-MCMC is larger in this case, compared to the Ricker model, since ADA-GP-MCMC is 4.6 times faster than MCWM, and 1.5 times faster than DA-GP-MCMC. For further analyses of the speed-up properties of ADA-GP-MCMC see Section 7.3, since these are very model dependent and the acceleration produced by ADA will increase if the likelihood function gets more and more intensive to evaluate. The algorithm efficiency measure min ESS/minute in Table 5 indicates that the the ADA-GP-MCMC is somewhat more efficient than both MCWM and DA-GP-MCMC. In Table 6 we present the estimated probabilities for the four different cases, and we can conclude that case 4 is the least likely case. We also notice that the performance of the selection algorithm is much better for case 2 than for case 4: this is due to the unbalance of the two classes, meaning that in our training data case 2 occur more frequently than case 4 and therefore it is more difficult to estimate the latter

case accurately.

7.2.2 Inference for protein folding data

We will now consider the protein folding data set 2 in Figure 4. The two parameters that are considered to be known are fixed to $A = -0.0025$ and $g = 0$. The remaining parameters are treated as unknown. Gaussian priors are set as follows: $\pi(\log \kappa) \sim \mathcal{N}(-0.7, 0.8^2)$, $\pi(\log \gamma) \sim \mathcal{N}(-0.7, 0.8^2)$, $\pi(\log c) \sim \mathcal{N}(3.34, 0.173^2)$, $\pi(\log d) \sim \mathcal{N}(2.3, 0.4^2)$, $\pi(\log p_1) \sim \mathcal{N}(0, 0.5^2)$, $\pi(\log p_2) \sim \mathcal{N}(0, 0.5^2)$, and $\pi(\log \sigma) \sim \mathcal{N}(0.69, 0.5^2)$. The starting parameter values were set to $\exp(\theta_0) = [0.5, 2, 20, 15, 1.5, 1.5, 2.5]$. Same as in Section 7.2.1, we use 250 particles to obtain four independent and unbiased approximations of the likelihood function, that we average to obtain another unbiased likelihood. The algorithm settings for the MCWM, DA-GP-MCMC, and ADA-GP-MCMC are the same as in the previous simulation study.

Marginal posteriors are in Figure 8, and inference results are in Table 7. Algorithmic properties can be found in Table 8, and we can conclude that we also in this case obtain a better speed-up compared to the speed-up that we obtain for the Ricker model. The estimated probabilities for the selection of the four different cases are in Table 9, and these are similar to the results reported in Section 7.2.1. Eight illustrative samples from the posterior predictive distribution (see Appendix B for how this distribution is computed) are presented in Figure 7. Each of the eight samples has been obtained using a parameter draw randomly picked from the MCMC chain after burn-in. The inference results for the protein folding data are similar to those produced for the simulated data in Section 7.2.1. We also notice that predicted trajectories in Figure 7 correspond very well with observed data. This indicates that our inference results are realistic.

Table 7: Parameter estimations (posterior mean and posterior quantile interval (2.5th and 97.5th quantile)) for MCWM, DA-GP-MCMC, and ADA-GP-MCMC.

	MCWM	DA-GP-MCMC	ADA-GP-MCMC
$\log \kappa$	0.73 [0.42,1.19]	0.74 [0.45,1.12]	0.76 [0.42,1.29]
$\log \gamma$	0.53 [0.45,0.59]	0.52 [0.44,0.6]	0.52 [0.44,0.59]
$\log c$	3.09 [3.08,3.11]	3.1 [3.08,3.1]	3.1 [3.08,3.11]
$\log d$	3.36 [2.94,3.84]	3.32 [2.89,3.89]	3.35 [2.91,3.81]
$\log p_1$	0.46 [0.35,0.57]	0.45 [0.34,0.58]	0.45 [0.34,0.56]
$\log p_2$	-0.08 [-0.26, 0.09]	-0.07 [-0.26,0.08]	-0.08 [-0.25,0.07]
$\log \sigma$	0.68 [0.56,0.8]	0.68 [0.57,0.78]	0.69 [0.57,0.82]

Table 8: Algorithm properties for the the MCWM, DA-GP-MCMC, and ADA-GP-MCMC algorithm.

	Min 1000 iter.	Acceptance rate (%)	min ESS/min	Second stage direct (%)	Early- rejections (%)
MCWM	75.88	18.5	0.39	NA	NA
DA-GP-MCMC	24.81	3.96	0.69	15.27	68.95
ADA-GP-MCMC	15.37	3.34	0.94	14.52	69.21

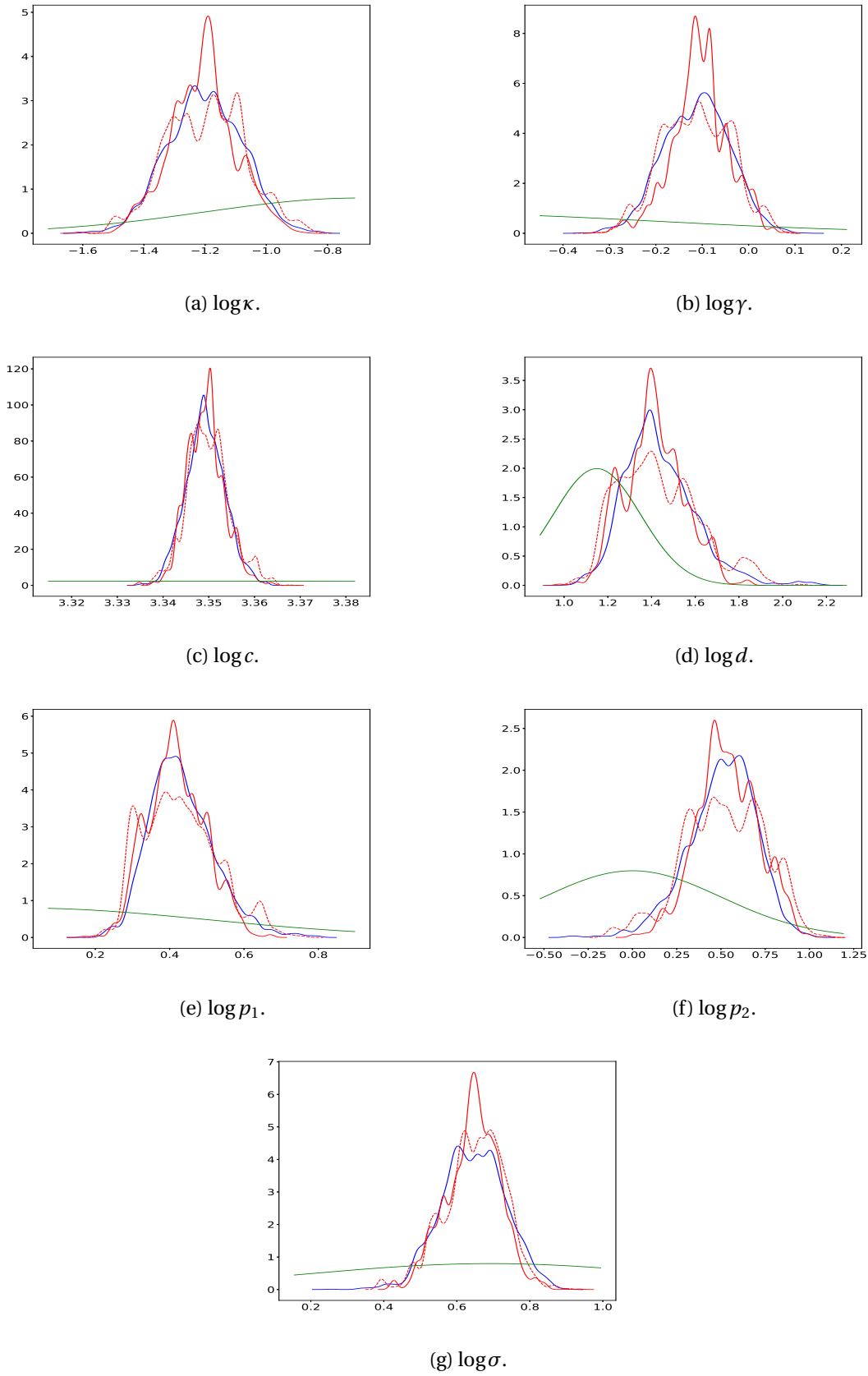
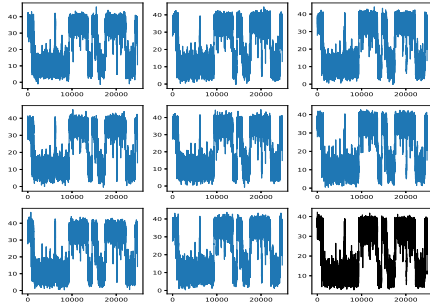


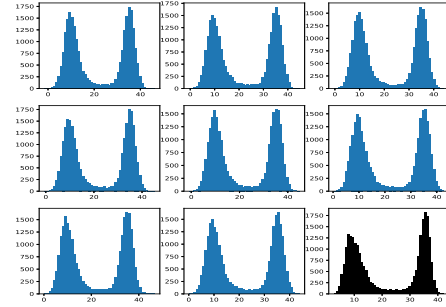
Figure 6: Marginal posteriors based on simulated data: MCWM (blue solid line), DA-GP-MCMC (red solid line), and ADA-GP-MCMC (red dashed line). Priors are denoted with green lines (these look “cut” as we zoom on the bulk of the posterior), and the true parameter values are marked with black vertical lines.

Table 9: Estimated probabilities for the different cases and percentage of times the assumption for the different cases in the ADA-GP-MCMC algorithm holds.

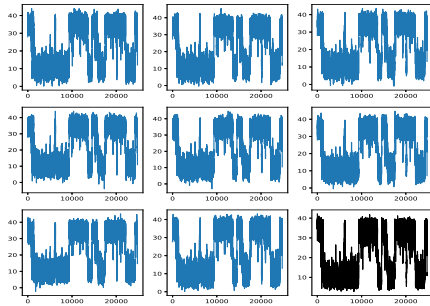
	Case 1	Case 2	Case 3	Case 4
Est. prob.	0.22	0.91	0.78	0.09
Perc. assum. holds	43.14	87.67	65.92	25.38



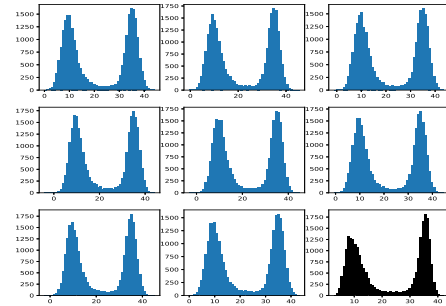
(a) Posterior predictives from MCWM.



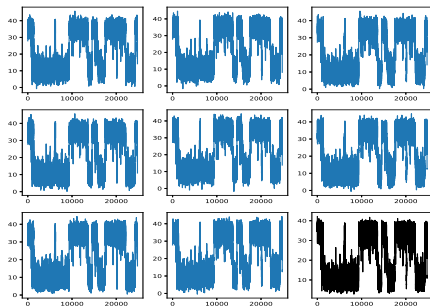
(b) Marginal predicted data from MCWM.



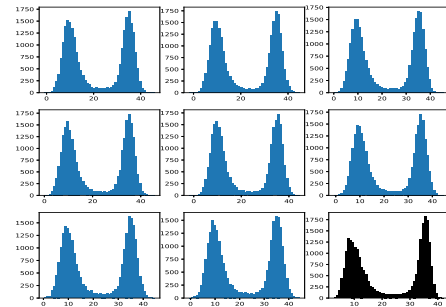
(c) Posterior predictives from DA-GP-MCMC.



(d) Marginal predicted data from DA-GP-MCMC.

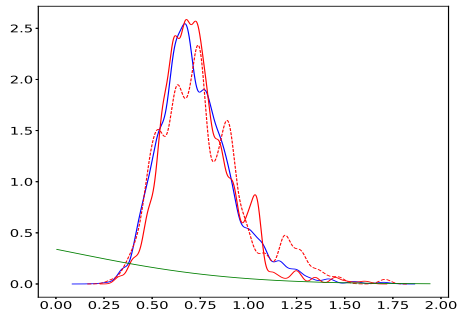


(e) Posterior predictives from ADA-GP-MCMC.

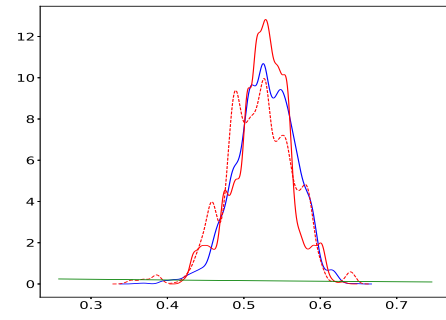


(f) Marginal predicted data from ADA-GP-MCMC.

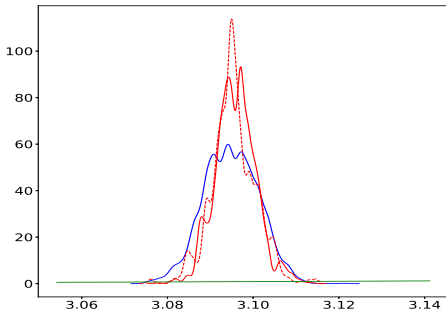
Figure 7: Trajectories sampled from the posterior predictive distribution (left), based on parameters drawn from MCWM, DA-GP-MCMC, and ADA-GP-MCMC. Corresponding marginal distributions (right). Samples from the posterior predictive distributions are in blue; real data are in black.



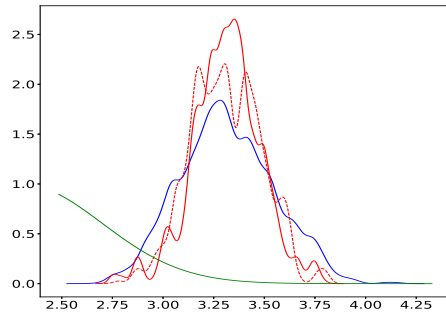
(a) $\log \kappa$.



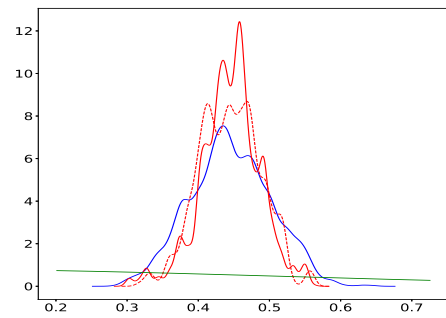
(b) $\log \gamma$.



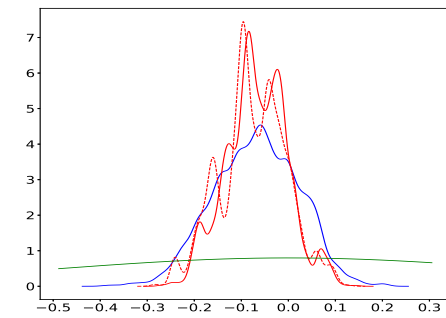
(c) $\log c$.



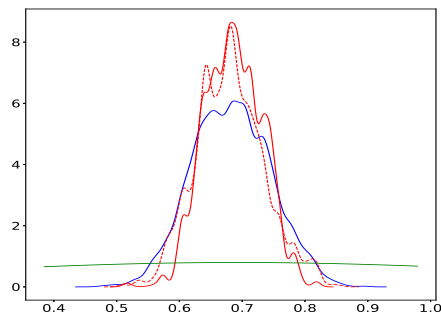
(d) $\log d$.



(e) $\log p_1$.



(f) $\log p_2$.



(g) $\log \sigma$.

Figure 8: Marginal posteriors based on protein folding data: MCWM (blue solid line), DA-GP-MCMC (red solid line), and ADA-GP-MCMC (red dashed line). Priors are denoted with green lines (these look “cut” as we zoom on the bulk of the posterior), and the true parameter values are marked with black vertical lines.

7.3 Analysis of ADA-GP-MCMC

In the following we simplify the notation and refer to ADA-GP-MCMC and DA-GP-MCMC as ADA and DA. To analyze the speed-up produced by the ADA algorithm we execute multiple runs of both DA and ADA. We focus on four metrics: runtimes for DA and ADA; the speed-up attained by ADA, expressed in how many times faster this is in comparison with DA; the number of particle filter evaluations in the second stage for DA and ADA (notice, in the DA case this corresponds exactly to the number of times the second stage is reached); the reduction in the number of particle filter evaluations for ADA compared to DA.

For the Ricker model, both algorithms are run independently for 100 times, and each run consists of 50,000 iterations. The algorithm settings were kept the same as in Section 7.1. The four metrics of the speed-up analysis are in Figure 9. From Figure 9c we notice that, by considering the MCMC iterations when the second stage is reached, ADA manages to avoid for about 500 times the evaluation of the particle filter. However, the speed-up for this specific model is low, since the execution of each particle filter is computationally cheap.

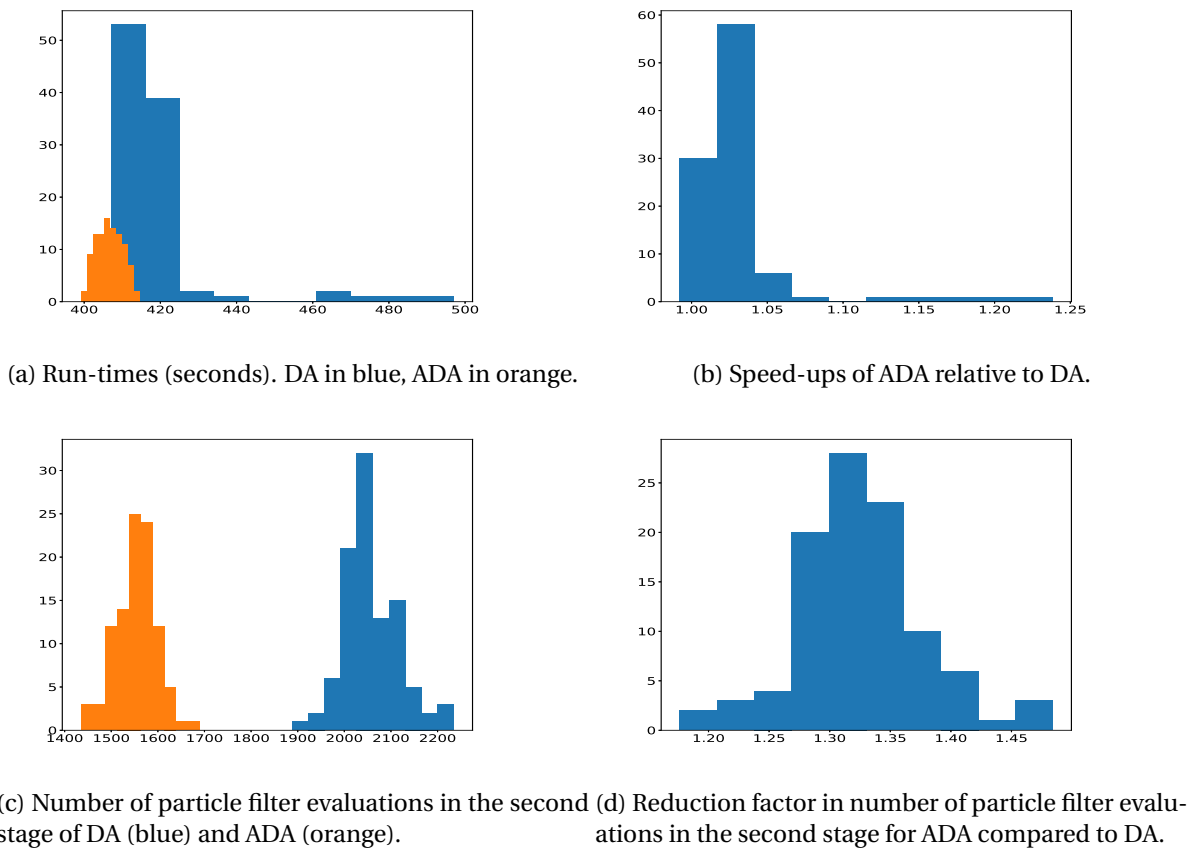
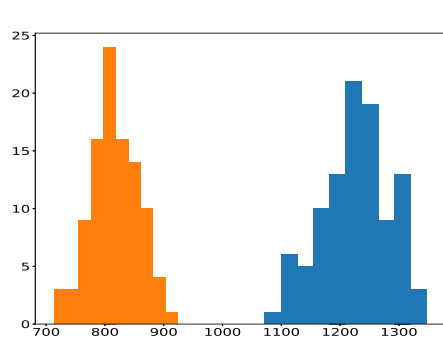


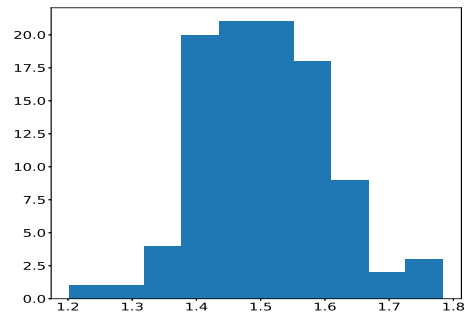
Figure 9: Speed-up analysis for the Ricker model across 100 independent simulations.

Also for the DWP-SDE model we independently execute DA and ADA for 100 times, on the simulated data set used in Section 7.2.1 and the protein folding data set considered in Section 7.2.2. For each instance, both algorithms are run for 1,000 iterations (since the analysis is very time consuming). Settings were kept the same as in Section 7.2.1 and 7.2.2, respectively. Run-times and number of particle filter evaluations are presented in Figure 10 and 11. As expected, compared to the less expensive Ricker model, here we obtain a more noticeable speed-up. This is because the expensive particle filter is invoked 2 to 6 times less often for ADA than for DA (Figure 10d and 11d). Clearly, it would be easy (at least in principle) to artificially enlarge the size of the analyzed data, to make the evaluation

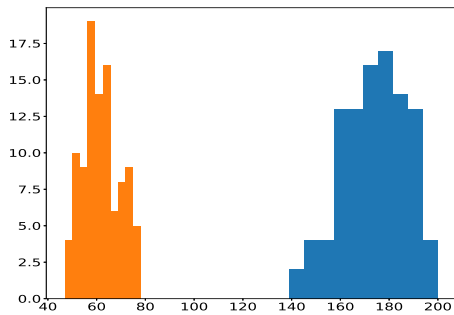
of the particle filter even more computationally intensive, so that the run times differences would be even more dramatic than those reported in Figures 10a and 11a.



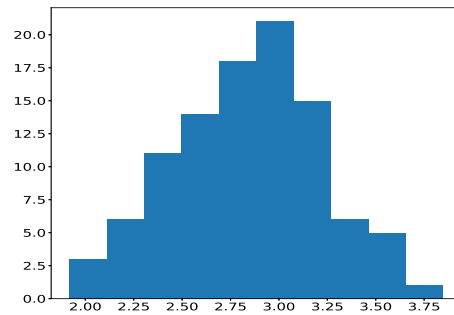
(a) Run-times (seconds). DA in blue, ADA in orange.



(b) Speed-ups of ADA relative to DA.



(c) Number of particle filter evaluations in the second stage of DA (blue) and ADA (orange).



(d) Reduction factor in number of particle filter evaluations in the second stage for ADA compared to DA.

Figure 10: Speed-up analysis across 100 independent simulations for the DWP model using the simulated data set.

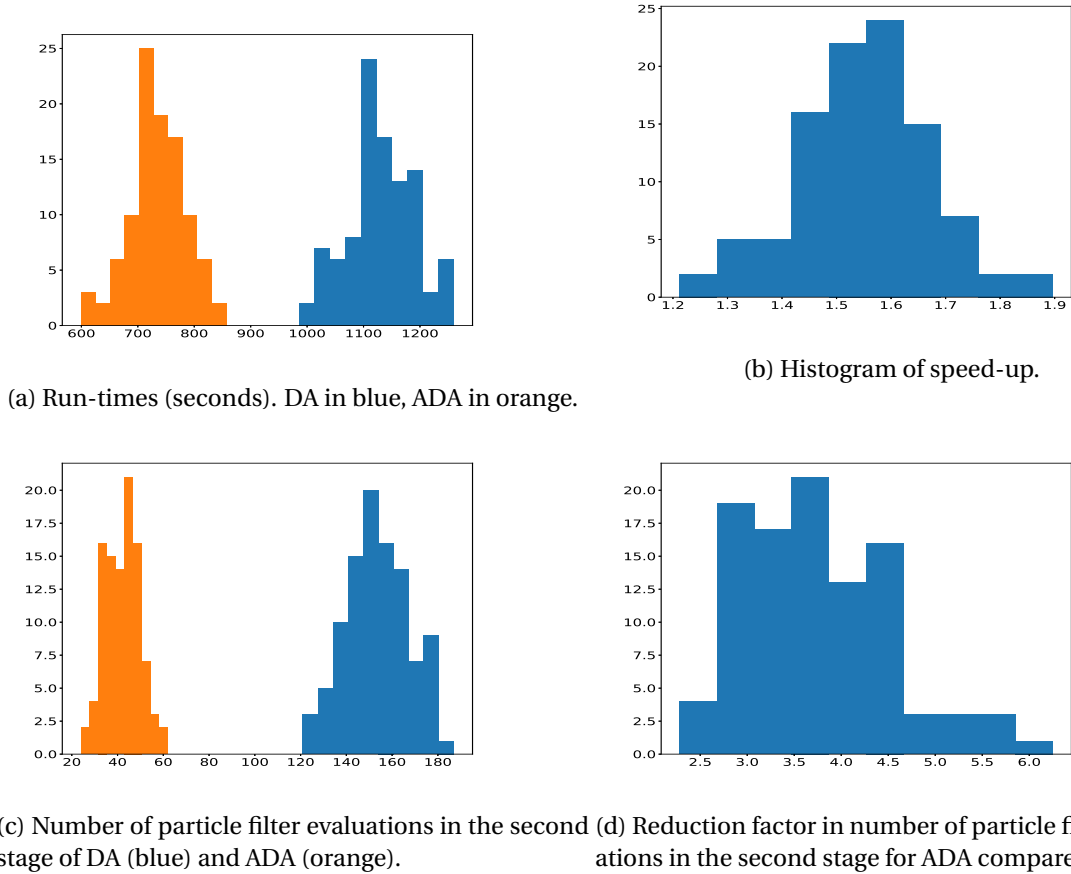


Figure 11: Speed-up analysis for the DWP model across 100 independent simulations using the protein folding data set.

Regarding ADA, it is interesting to study how often each of the four possible cases illustrated in Section 2.1 are selected, and how likely it is that we run a particle filter conditionally on the selected case. Table 10 reports our findings for the Ricker model and the DWP-SDE model on simulated and real data. We notice that proposals are not equally likely to be sent to each of the four cases, and that case 4 is the least likely case for a proposal to be sent to. It is perhaps surprising to observe the marked difference in the percentages of proposals sent to case 3 and case 4, as both cases correspond to likelihood ratios (ratio of GP likelihoods and ratio of particle filter likelihoods) that disagree in sign at the evaluated proposal. Furthermore, we can also conclude that the probability of running the particle filter varies for the different cases. Not surprisingly, given how the cases are defined, the probability for case 2 is 1 and is 0 for case 4. We also note that the probability of running the particle filter in case 3 is much lower compared to case 1: this means that whenever case 1 is selected for proposal θ^* it turns that the event $u < \tilde{L}(\theta^{r-1})/\tilde{L}(\theta^*)$ is less likely than the event having the opposite inequality. If instead case 3 is selected, event $u > \tilde{L}(\theta^{r-1})/\tilde{L}(\theta^*)$ is less likely than the event having the opposite inequality.

Table 10: Percentage of proposals sent to the different cases (mean over 100 iterations of the ADA-MCMC algorithm), and probability of running the particle filter given the specific selected case (mean over 100 iterations of the ADA-MCMC algorithm).

	Percentage of proposals in each case				Prob. of running particle filter in each case			
	Case 1	Case 2	Case 3	Case 4	Case 1	Case 2	Case 3	Case 4
Ricker model	62.59	12.61	21.31	3.59	0.82	1	0.40	0
DWP-SDE simulated data.	17.85	13.60	66.35	2.21	0.97	1	0.04	0
DWP-SDE protein folding data.	18.80	6.82	73.28	1.09	0.98	1	0.024	0

8 Summary

We have provided ways to speed up MCMC sampling by introducing a novel, approximate version of the so-called “delayed-acceptance” MCMC first introduced in [Christen and Fox \[2005\]](#). More specifically, our ADA-MCMC algorithm (ADA standing for accelerated-approximated delayed-acceptance), can be used to accelerate MCMC sampling for Bayesian inference by exploiting possibilities to avoid the evaluation of the (possibly computationally expensive) likelihood function. While the standard DA-MCMC only accepts proposals by evaluating the likelihood function associated to the exact posterior, instead ADA-MCMC in some specific cases can accept parameter proposals even without the evaluation of the likelihood. Clearly, this is particularly relevant in statistical experiments where the likelihood function is not analytically available and is expensive to approximate. This is typical when unbiased approximations of the likelihood are used in pseudo-marginal algorithms for exact Bayesian inference [[Andrieu and Roberts, 2009](#)]. Another situation where ADA-MCMC comes useful is when the likelihood function turns expensive due to the size of the data.

Both DA-MCMC and ADA-MCMC depend on the construction of surrogates of the likelihood function, to be used in place of the latter when the evaluation of the true likelihood is to be avoided in a Metropolis-Hastings step. Unfortunately, producing a useful (i.e. informative) surrogate of the likelihood has its own cost. In fact, the construction of the surrogate model is typically the result of a “learning” procedure, where the output of a preliminary MCMC run (obtained using the expensive likelihood) is used to understand the relationship between simulated parameters and simulated data (e.g. using neuronal-networks as in [Papamakarios et al., 2018](#)), or between simulated loglikelihoods and parameter proposals (as in [Drovandi et al., 2018](#)). The preliminary MCMC will of course be computationally expensive, and in this work we do not propose strategies to alleviate this problem, as ADA-MCMC only accelerate MCMC sampling provided a surrogate model has already been obtained. For large datasets of independent measurements, there are “subsampling methods” that could be used to provide training data for the surrogate model, at a discounted cost ([Ahn et al., 2012](#), [Korattikara et al., 2014](#)). However we are not in general focusing on independent measurements.

ADA-MCMC samples from an approximate posterior distribution, while the original DA-MCMC algorithm is an exact algorithm. However, our case studies suggest that the approximative posterior inference returned by ADA-MCMC is close to the one obtained with DA-MCMC and Markov-chain-within-Metropolis (MCWM). However, this result is possibly connected with the quality of the surrogate model. If a poor surrogate model was used, the inference obtained using ADA-MCMC could be biased compared to DA-MCMC. The reason for this is that, in some cases, ADA-MCMC allows us to accept a proposal merely based on the surrogate model, while in DA-MCMC the likelihood function associated with the true posterior must be evaluated in order to accept a proposal.

As already mentioned, the main feature of the ADA-MCMC algorithm is its ability to avoid (when

possible) the evaluation of the likelihood function associated with the true posterior. This means that ADA-MCMC only generates an acceleration in the computations if the evaluation of the likelihood associated with the true posterior is time-consuming. If this evaluation is relatively fast, ADA-MCMC does not bring any significant gain compared to DA-MCMC. An example of the latter case is shown with the Ricker model case study, where we do not achieve any significant acceleration despite the fact that ADA-MCMC uses fewer evaluations of the particle filter compared to DA-MCMC. However, for the DWP-SDE model, each likelihood evaluation using a particle filter requires about 2 seconds and the benefits of using our novel approach are clear. Also, for this specific application, the expensive particle filter is invoked 2 to 6 times less often for ADA-MCMC than for DA-MCMC.

The ADA-MCMC algorithm is not limited to the Bayesian setting and can be used to sample from a generic distribution, as mentioned in Section 2.1. Furthermore, when considering the inference problem in a Bayesian setting, ADA-MCMC can straightforwardly be paired with some other surrogate model than the Gaussian process regression model we employ. Hence, ADA-MCMC is a general algorithm for Monte Carlo sampling that can be exploited in multiple ways, other than the ones we have illustrated.

Acknowledgements

Research was partially supported by the Swedish Research Council (VR grant 2013-05167). We thank Prof. Kresten Lindorff-Larsen (Copenhagen Biocenter, University of Copenhagen) and Dr. Wouter Boomsma (Computer Science, University of Copenhagen) for providing data for the protein-folding case study and for inspiring discussions on the topic.

References

- S. Ahn, A. Korattikara, and M. Welling. Bayesian posterior sampling via stochastic gradient Fisher scoring. In *Proceedings of the 29th International Conference on Machine Learning*, pages 1771–1778, 2012.
- C. Andrieu and G. O. Roberts. The pseudo-marginal approach for efficient Monte Carlo computations. *The Annals of Statistics*, 37:697–725, 2009.
- C. Andrieu and J. Thoms. A tutorial on adaptive MCMC. *Statistics and Computing*, 18(4):343–373, 2008.
- C. Andrieu, A. Doucet, and R. Holenstein. Particle Markov chain Monte Carlo methods. *Journal of the Royal Statistical Society: Series B (Statistical Methodology)*, 72(3):269–342, 2010.
- E. Angelino, M. J. Johnson, R. P. Adams, et al. Patterns of scalable Bayesian inference. *Foundations and Trends® in Machine Learning*, 9(2-3):119–247, 2016.
- M. Banterle, C. Grazian, A. Lee, and C. P. Robert. Accelerating metropolis-hastings algorithms by delayed acceptance. *arXiv preprint arXiv:1503.00996*, 2015.
- M. A. Beaumont. Estimation of population growth or decline in genetically monitored populations. *Genetics*, 164(3):1139–1160, 2003.
- J. Bezanson, A. Edelman, S. Karpinski, and V. Shah. Julia: A fresh approach to numerical computing. *SIAM Review*, 59(1):65–98, 2017.
- O. Cappé, E. Moulines, and T. Ryden. *Inference in Hidden Markov Models*. Springer, 2005.
- O. Cappé, S. J. Godsill, and E. Moulines. An overview of existing methods and recent advances in sequential Monte Carlo. *Proceedings of the IEEE*, 95(5):899–924, 2007.

- J. A. Christen and C. Fox. Markov chain Monte Carlo using an approximation. *Journal of Computational and Graphical statistics*, 14(4):795–810, 2005.
- P. Das, M. Moll, H. Stamati, L. E. Kaviraki, and C. Clementi. Low-dimensional, free-energy landscapes of protein-folding reactions by nonlinear dimensionality reduction. *Proceedings of the National Academy of Sciences*, 103(26):9885–9890, 2006.
- C. C. Drovandi. Pseudo-marginal algorithms with multiple CPUs. <https://eprints.qut.edu.au/61505/>, 2014.
- C. C. Drovandi, M. T. Moores, and R. J. Boys. Accelerating pseudo-marginal MCMC using Gaussian processes. *Computational Statistics & Data Analysis*, 118:1–17, 2018.
- R. G. Everitt and P. A. Rowińska. Delayed acceptance ABC-SMC. *arXiv:1708.02230*, 2017.
- S.-C. Fang, D. Y. Gao, G.-X. Lin, R.-L. Sheu, and W.-X. Xing. Double well potential function and its optimization in the n -dimensional real space: part i. *Journal of Industrial and Management Optimization*, 13(3):1291–1305, 2017.
- M. Fasiolo, N. Pya, and S. Wood. A comparison of inferential methods for highly nonlinear state space models in ecology and epidemiology. *Statistical Science*, 31(1):96–118, 2016.
- P. Fearnhead and D. Prangle. Constructing summary statistics for approximate Bayesian computation: semi-automatic approximate Bayesian computation. *Journal of the Royal Statistical Society: Series B*, 74(3):419–474, 2012.
- J. L. Forman and M. Sørensen. A transformation approach to modelling multi-modal diffusions. *Journal of Statistical Planning and Inference*, 146:56–69, 2014.
- J. Franks and M. Vihola. Importance sampling and delayed acceptance via a Peskun type ordering. *arXiv:1706.09873*, 2017.
- J. Gabry, D. Simpson, A. Vehtari, M. Betancourt, and A. Gelman. Visualization in Bayesian workflow. *arXiv preprint arXiv:1709.01449*, 2017.
- A. Gelman, J. B. Carlin, H. S. Stern, D. B. Dunson, A. Vehtari, and D. B. Rubin. *Bayesian data analysis*, volume 2. CRC press Boca Raton, FL, 2014.
- A. Golightly, D. A. Henderson, and C. Sherlock. Delayed acceptance particle MCMC for exact inference in stochastic kinetic models. *Statistics and Computing*, 25(5):1039–1055, 2015.
- N. J. Gordon, D. J. Salmond, and A. F. Smith. Novel approach to nonlinear/non-gaussian bayesian state estimation. In *IEE Proceedings F (Radar and Signal Processing)*, volume 140, pages 107–113. IET, 1993.
- W. K. Hastings. Monte Carlo sampling methods using Markov chains and their applications. *Biometrika*, 57(1):97–109, 1970.
- P. E. Jacob. Sequential Bayesian inference for implicit hidden Markov models and current limitations. *ESAIM: Proceedings and Surveys*, 51:24–48, 2015.
- N. Kantas, A. Doucet, S. S. Singh, J. Maciejowski, and N. Chopin. On particle methods for parameter estimation in state-space models. *Statistical Science*, 30(3):328–351, 2015.
- G. Karabatsos and F. Leisen. An approximate likelihood perspective on ABC methods. Forthcoming in *Statistics Surveys*. Also available as *arXiv:1708.05341*, 2017.

- G. Kitagawa. Monte Carlo filter and smoother for non-gaussian nonlinear state space models. *Journal of computational and graphical statistics*, 5(1):1–25, 1996.
- A. Korattikara, Y. Chen, and M. Welling. Austerity in MCMC land: Cutting the Metropolis-Hastings budget. In *International Conference on Machine Learning*, pages 181–189, 2014.
- J. Marin, P. Pudlo, C. Robert, and R. Ryder. Approximate Bayesian computational methods. *Statistics and Computing*, pages 1–14, 2012.
- F. J. Medina-Aguayo, A. Lee, and G. O. Roberts. Stability of noisy Metropolis–Hastings. *Statistics and Computing*, 26:1187–1211, 2016.
- E. Meeds and M. Welling. GPS-ABC: Gaussian process surrogate approximate Bayesian computation. In *Proceeding of the 30th conference on Uncertainty in Artificial Intelligence (UAI)*, 2014.
- C. L. Mueller. Exploring the common concepts of adaptive MCMC and covariance matrix adaptation schemes. In A. Auger, J. L. Shapiro, L. D. Whitley, and C. Witt, editors, *Theory of Evolutionary Algorithms*. Schloss Dagstuhl - Leibniz-Zentrum für Informatik, Germany, 2010.
- K. P. Murphy. *Machine learning: a probabilistic perspective*. MIT press, 2012.
- G. Papamakarios, D. C. Sterratt, and I. Murray. Sequential neural likelihood: Fast likelihood-free inference with autoregressive flows. *arXiv preprint arXiv:1805.07226*, 2018.
- U. Picchini. Inference for SDE models via approximate Bayesian computation. *Journal of Computational and Graphical Statistics*, 23(4):1080–1100, 2014.
- U. Picchini and J. L. Forman. Accelerating inference for diffusions observed with measurement error and large sample sizes using approximate Bayesian computation. *Journal of Statistical Computation and Simulation*, 86(1):195–213, 2016.
- M. K. Pitt, R. dos Santos Silva, P. Giordani, and R. Kohn. On some properties of Markov chain Monte Carlo simulation methods based on the particle filter. *Journal of Econometrics*, 171(2):134–151, 2012.
- M. Quiroz, M.-N. Tran, M. Villani, and R. Kohn. Speeding up MCMC by delayed acceptance and data subsampling. *Journal of Computational and Graphical Statistics*, 2017. doi: 10.1080/10618600.2017.1307117.
- C. E. Rasmussen and C. K. I. Williams. *Gaussian processes for machine learning*. MIT press, 2006.
- J. Rosenthal and G. Roberts. Coupling and ergodicity of adaptive MCMC. *Journal of Applied Probability*, 44:458–475, 2007.
- C. Sherlock, A. H. Thiery, G. O. Roberts, J. S. Rosenthal, et al. On the efficiency of pseudo-marginal random walk Metropolis algorithms. *The Annals of Statistics*, 43(1):238–275, 2015.
- C. Sherlock, A. Golightly, and D. A. Henderson. Adaptive, delayed-acceptance MCMC for targets with expensive likelihoods. *Journal of Computational and Graphical Statistics*, 26(2):434–444, 2017.
- S. Sisson and Y. Fan. *Handbook of Markov Chain Monte Carlo*, chapter Likelihood-free MCMC. Chapman & Hall/CRC, New York.[839], 2011.
- A. Solonen, P. Ollinaho, M. Laine, H. Haario, J. Tamminen, and H. Järvinen. Efficient MCMC for climate model parameter estimation: parallel adaptive chains and early rejection. *Bayesian Analysis*, 7(3):715–736, 2012.

R. Tibshirani. Regression shrinkage and selection via the lasso. *Journal of the Royal Statistical Society. Series B*, pages 267–288, 1996.

S. N. Wood. Statistical inference for noisy nonlinear ecological dynamic systems. *Nature*, 466(7310): 1102–1104, 2010.

A Diagnostics for the GP model and selection methods

For diagnostic purposes of the predictive accuracy of the fitted models (GP and selection methods $s_{13}()$ and $s_{24}()$), we can split the *training* data, to obtain *testing* data. Basically, what we have denoted as \mathcal{D} and $\tilde{\mathcal{D}}$, can be partitioned as $\mathcal{D} = [\mathcal{D}_1, \mathcal{D}_2]$ and $\tilde{\mathcal{D}} = [\tilde{\mathcal{D}}_1, \tilde{\mathcal{D}}_2]$. Then \mathcal{D}_1 (and $\tilde{\mathcal{D}}_1$) can be used to fit the GP model, while \mathcal{D}_2 (and $\tilde{\mathcal{D}}_2$) is the “test data”, which is not used to fit the GP model, nor to fit the selection methods. Instead the test data is merely used to evaluate the performance of the GP model and the selection methods, as typically done with predictive models. In this case by considering data that is not used to fit the GP model.

To test the fit of the GP model, we predict likelihood values from the GP for each proposal in the test data in \mathcal{D}_2 , and compare the GP predictions to the corresponding particle filter predictions that are stored in \mathcal{D}_2 .

Testing the performance of the selection methods is a slightly more involved process. For each proposal in the test data \mathcal{D}_2 we compute corresponding GP predictions, and we also compute a new set of particle filter predictions. We then use the GP predictions and check if proposal r belongs to case 1 and 3, or case 2 and 4. Assume that proposal $\theta^{*,r}$ belongs to case 1 and 3. Then run the selection method $s_{1,3}(\theta^{*,r})$ for proposal r , and check which case proposal r belongs to. After having determined which case proposal r belongs to, according to the selection method, we check if the same case is selected using the new particle filter predictions, where we use the definition of the four cases in Section 2.1 to determine which case we should select, according to the new particle filter predictions. Using this method we can calculate how likely it is that the new particle filter predictions and the selection method are consistent.

B Evaluating the inference quality

While the Ricker model studied in Section 7.1 is a simulation study, where the ground-truth parameters used to generate “observed” data are known, it is easy to evaluate the quality of approximate inference methods. This is not the case for the study in Section 7.2, since ground-truth parameters are unknown for the considered protein folding data. For this case, we can make use of realizations from the posterior predictive distribution (e.g. Gelman et al. [2014] chapter 6). For given data z (using the notation in Section 7.2), the posterior predictive distribution is given by

$$p(z^*|z) = \int p(z^*|\theta)\pi(\theta|z)d\theta.$$

This is the distribution of data generated from the model, after having updated our beliefs about the model parameters by means of Bayes’ theorem [Gabry et al., 2017]. Furthermore, if the model fits the data well, most of samples z^* from the posterior predictive distribution should correspond well with the data z .

However, sampling from the posterior distribution for the model in (14) is not quite straightforward since the true likelihood $p(z|\theta)$ is not known. However, we can sample from an approximation of the posterior predictive distribution for model (14) using the following procedure. We pick a θ from the posterior samples of $\pi(\theta|z)$ that we have obtained from MCWM (or some other algorithm). The next step is to run the bootstrap filter based on θ , and once the filter has reached the last time point $t = T$ we sample a single particle x_T^k at random from the particles $x_T^{1:N}$, according to

corresponding probabilities $\tilde{w}_T^{1:N}$. We then use the genealogy for particle x_T^k (which we have stored) to reconstruct the path of $x_{1:T}^k$ backward. This resulting path is now denoted x^* . After computing x^* we independently generate a path y^* , by exactly sampling from its solution. Finally, to produce the wanted realization z^* , we simply add up the x^* path and the y^* path.

Supplementary material

Here we show some material pertaining our simulation and data analysis studies. We first report material pertaining the first application (stochastic Ricker model, see Section 7.1 of the main text) then the second application (Section 7.2 of the main text).

Thereafter, quantities denoted as “residuals” are computed as:

$$r_i = \ell_{PF}(\theta^{*,i}) - \ell_{GP}(\theta^{*,i}), \quad i = 1, \dots, N_{test}$$

where N_{test} is the number of observations in the test data \mathcal{D}_2 .

Ricker model

Here follow trace plots for MCMC chains obtained under different methods.

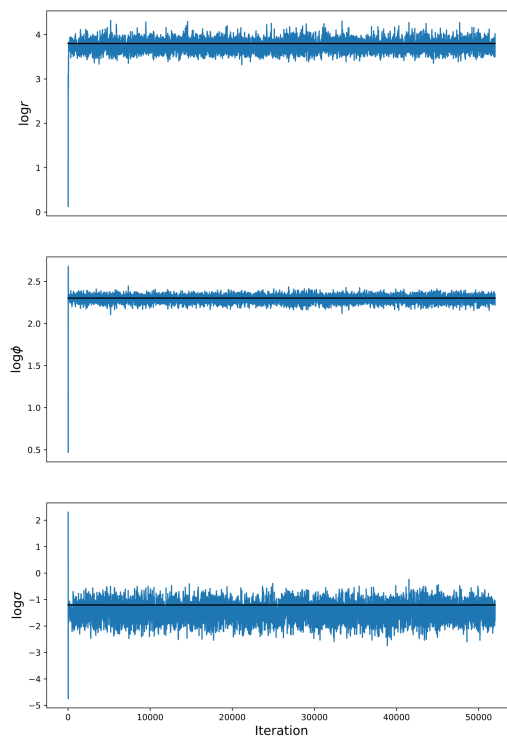


Figure 12: Trace plot for PMCMC. Horizontal lines denote the ground-truth parameter values.

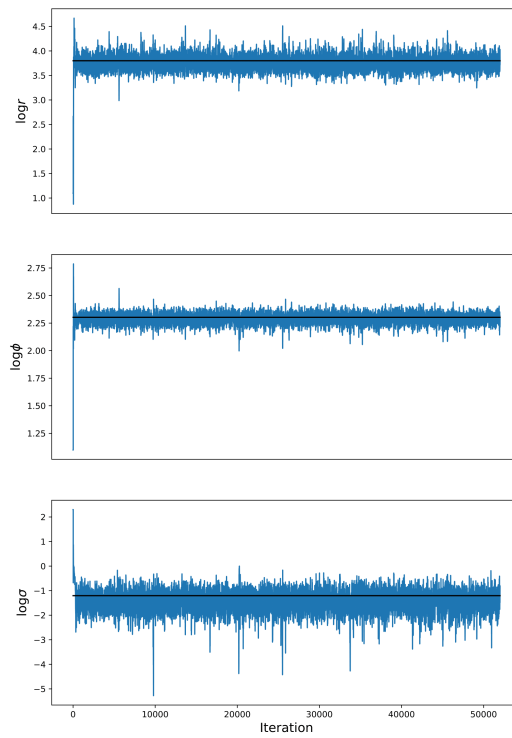


Figure 13: Trace plot for MCWM. Horizontal lines denote the ground-truth parameter values.

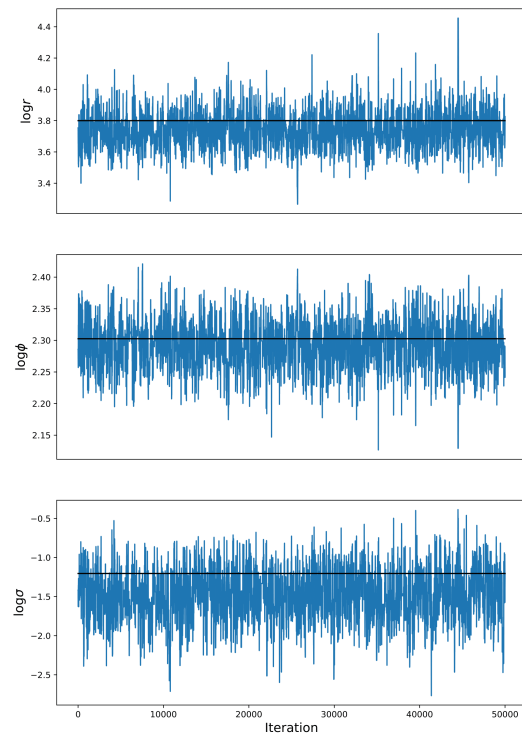


Figure 14: Trace plot for DA-GP-MCMC. Horizontal lines denote the ground-truth parameter values.

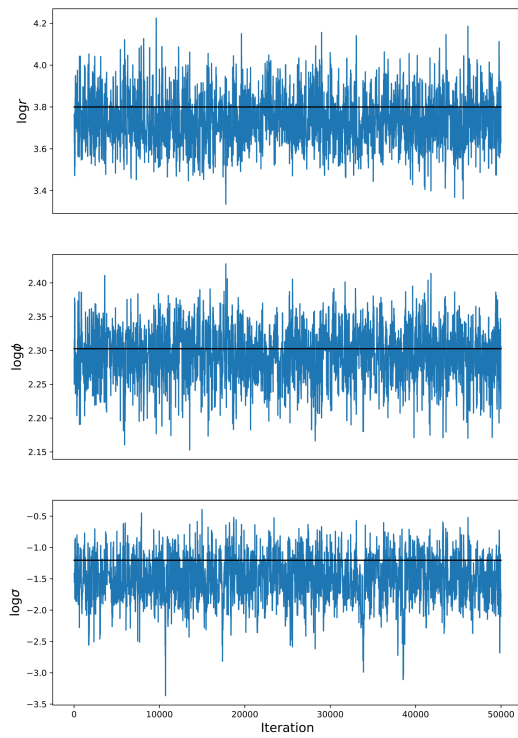


Figure 15: Trace plot for ADA-GP-MCMC. Horizontal lines denote the ground-truth parameter values.

Here follow some diagnostics pertaining the fit of the GP model.

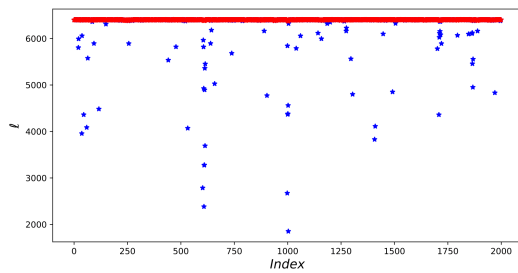


Figure 16: Log-likelihood estimations; particle filter (blue), Gaussian process model (red).

Residual plots.

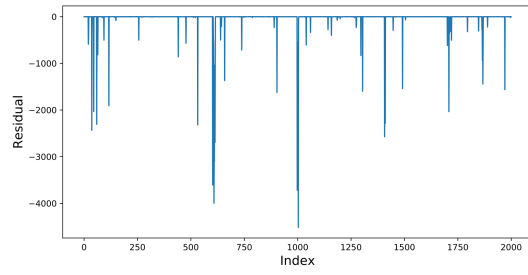
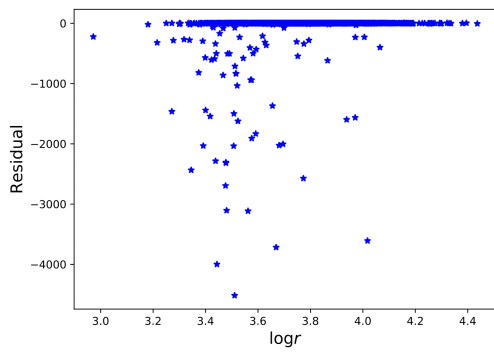
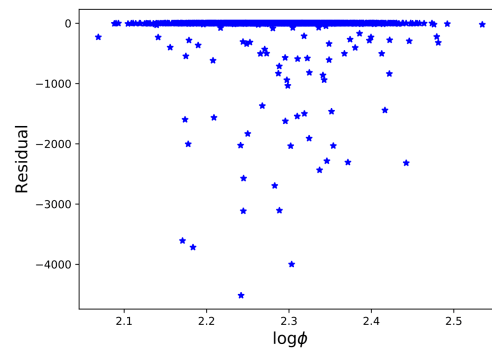


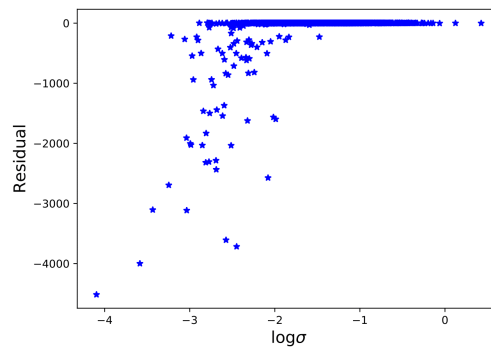
Figure 17: Residuals.



(a) Residuals vs. $\log r$.



(b) Residuals vs. $\log \phi$.



(c) Residuals vs. $\log \sigma$.

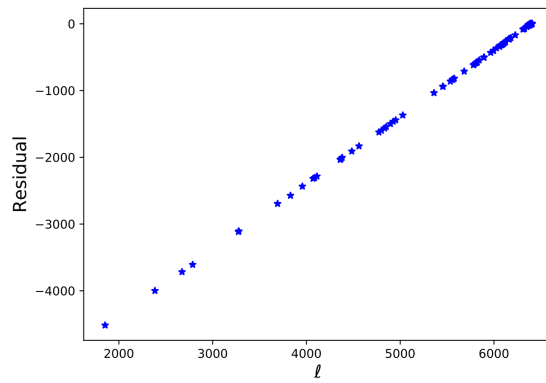


Figure 19: Residuals vs. $\hat{\ell}_{PF}$.

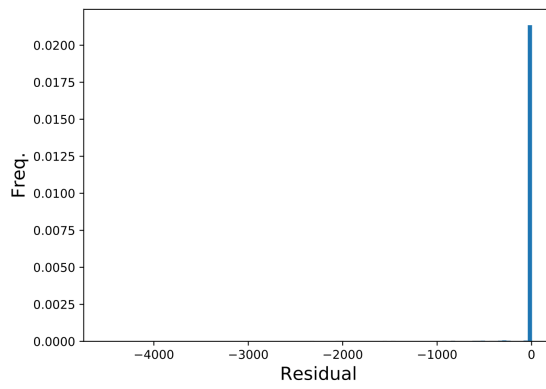


Figure 20: Histogram of residuals.

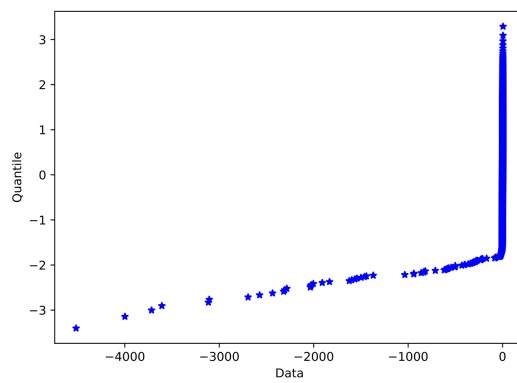


Figure 21: Normal probability plot of residuals.

DWP-SDE model for simulated data

Here follow trace plots for MCMC chains obtained under different methods.

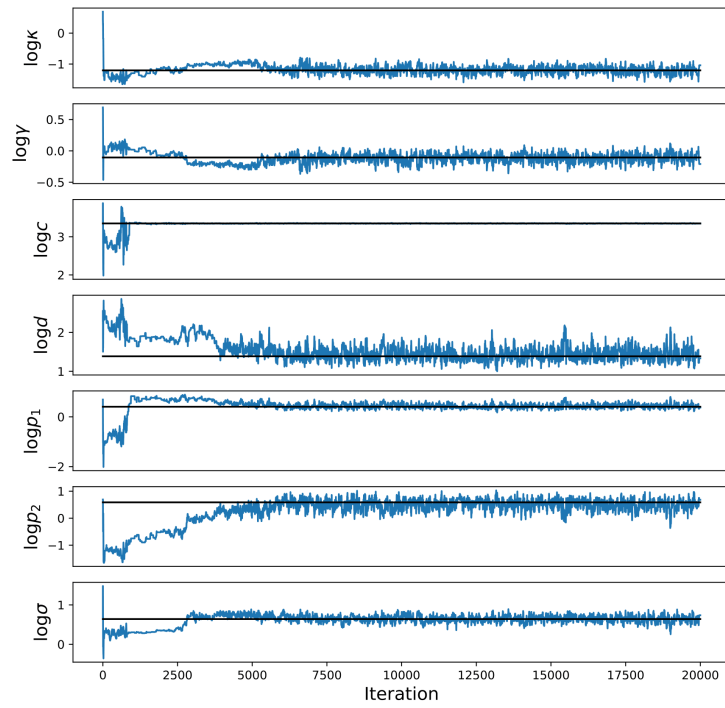


Figure 22: Trace plot for MCWM. Horizontal lines denote the ground-truth parameter values.

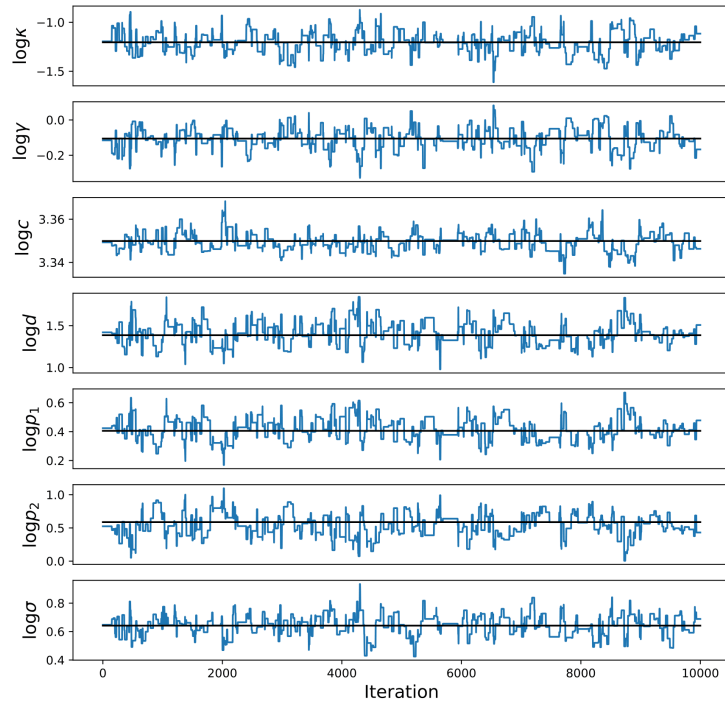


Figure 23: Trace plot for DA-GP-MCMC. Horizontal lines denote the ground-truth parameter values.

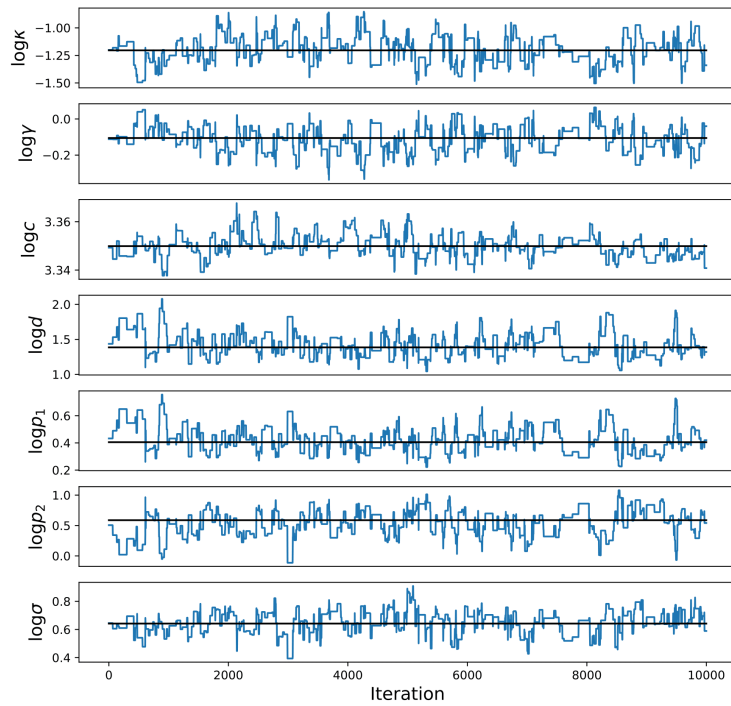


Figure 24: Trace plot for ADA-GP-MCMC. Horizontal lines denote the ground-truth parameter values.

Fit of the GP model.

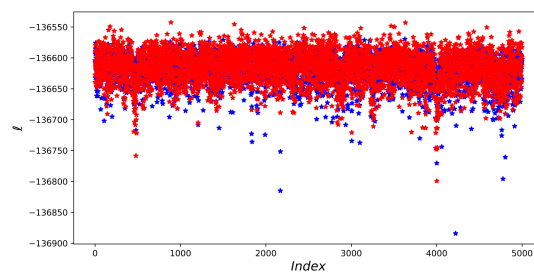


Figure 25: Log-likelihood estimations; particle filter (blue), Gaussian process model (red).

Residual plots.

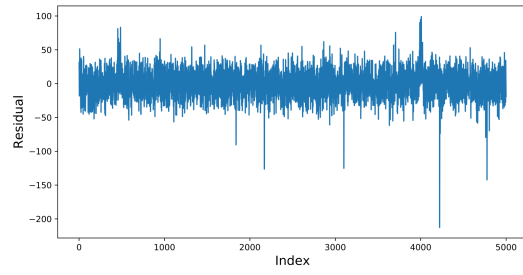
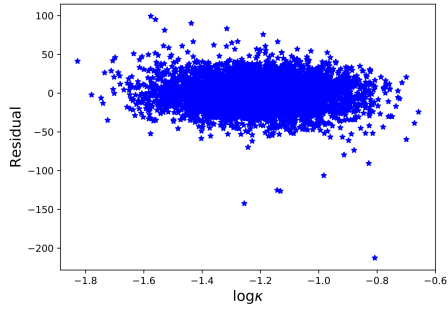
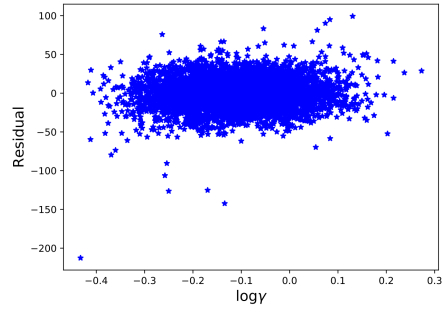


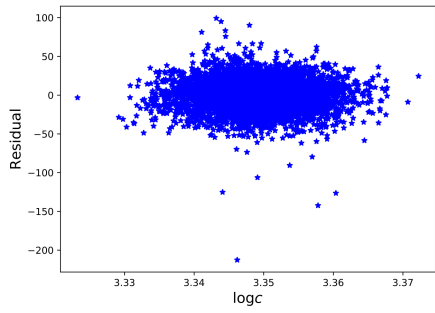
Figure 26: Residuals.



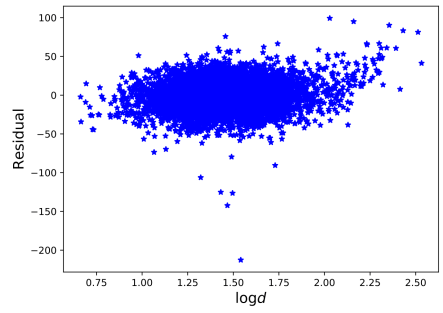
(a) Residuals vs. $\log \kappa$.



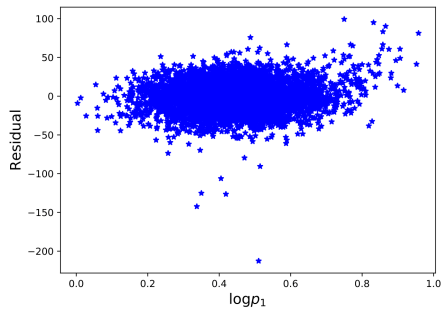
(b) Residuals vs. $\log \gamma$.



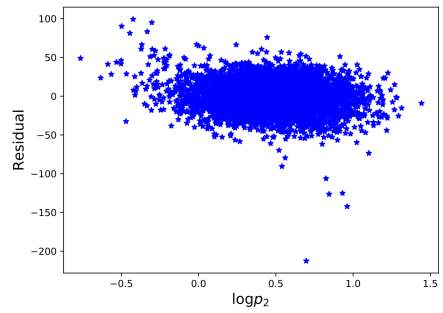
(c) Residuals vs. $\log c$.



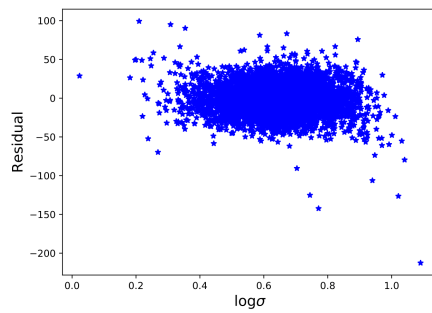
(d) Residuals vs. $\log d$.



(e) Residuals vs. $\log p_1$.



(f) Residuals vs. $\log p_2$.



(g) Residuals vs. $\log \sigma$.

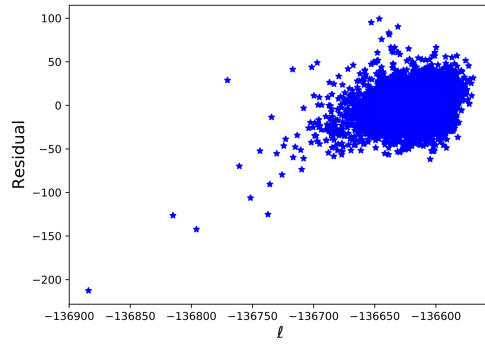


Figure 28: Residuals vs. $\hat{\ell}_{PF}$.

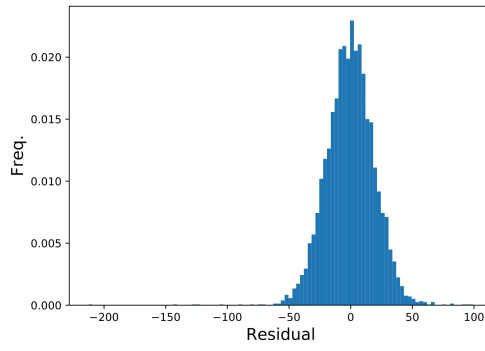


Figure 29: Histogram of residuals.

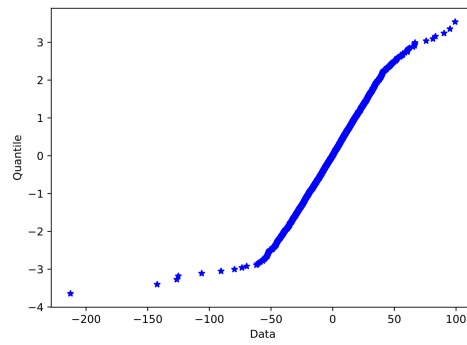


Figure 30: Normal probability plot for residuals.

DWP-SDE model for protein folding data

Here follow trace plots for MCMC chains obtained under different methods.

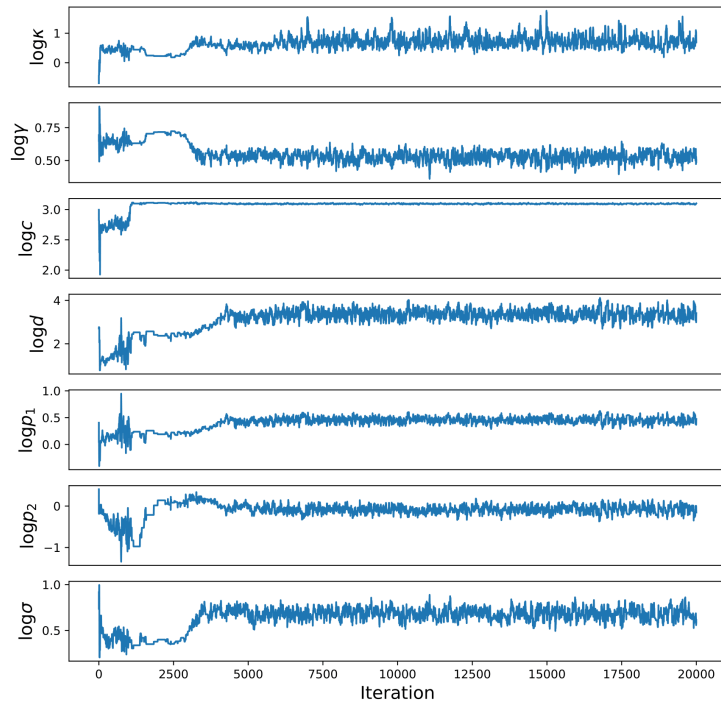


Figure 31: Trace plot for MCWM.

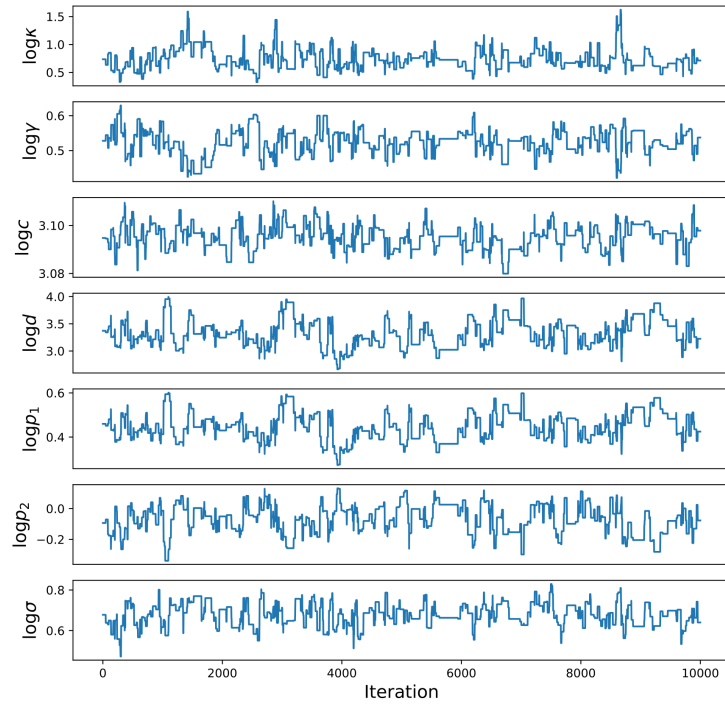


Figure 32: Trace plot for DA-GP-MCMC.

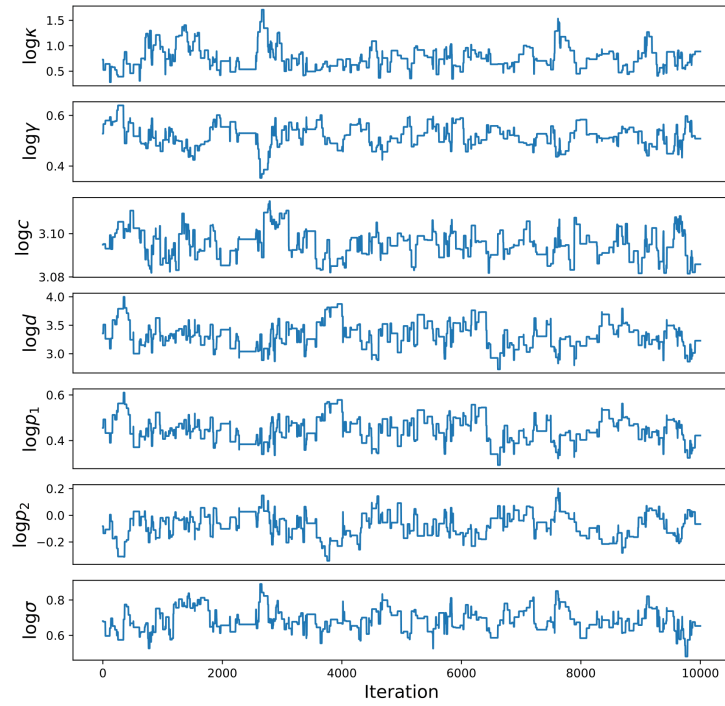


Figure 33: Trace plot for ADA-GP-MCMC.

Fit of the GP model.

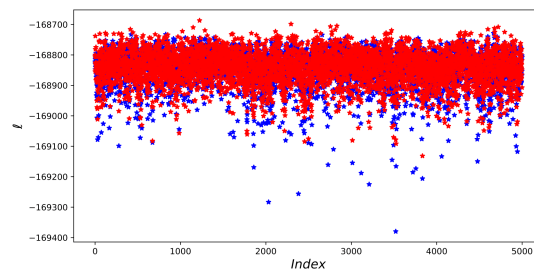


Figure 34: Log-likelihood estimations; particle filter (blue), Gaussian process model (red).

Residual plots.

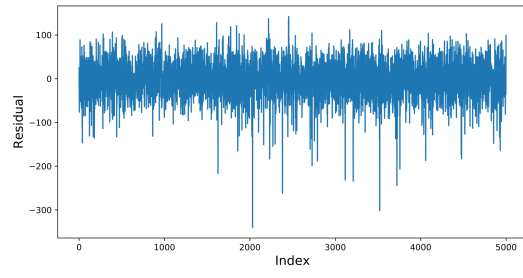
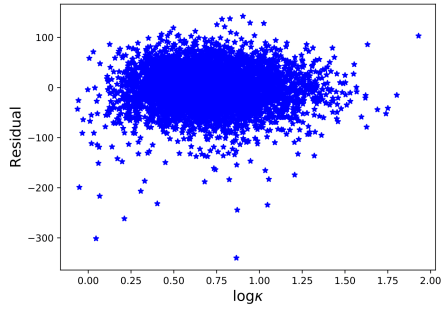
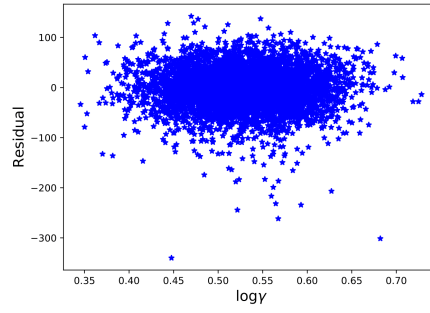


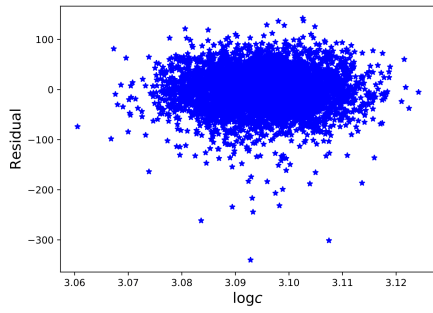
Figure 35: Residuals.



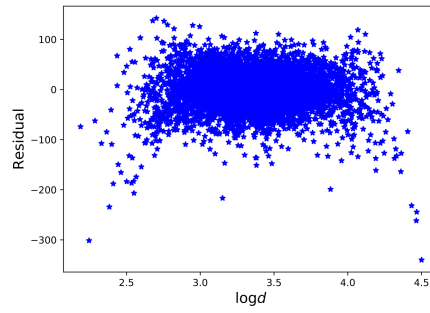
(a) Residuals vs. $\log \kappa$.



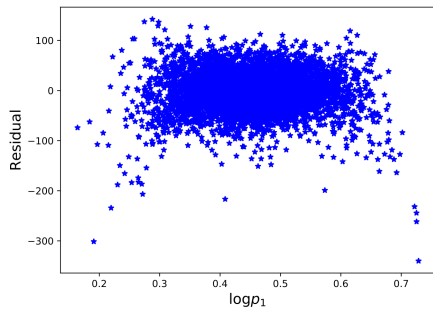
(b) Residuals vs. $\log \gamma$.



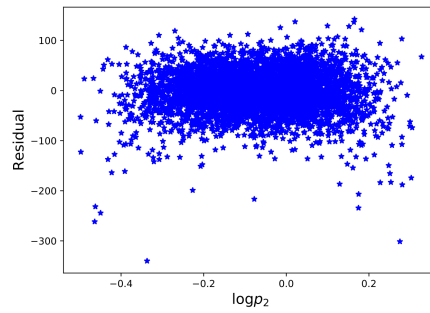
(c) Residuals vs. $\log c$.



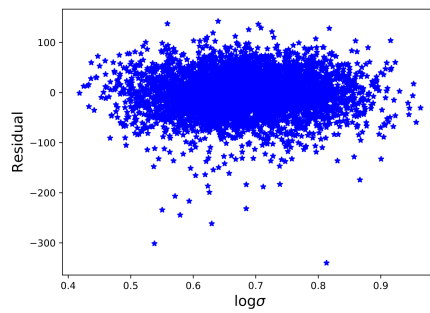
(d) Residuals vs. $\log d$.



(e) Residuals vs. $\log p_1$.



(f) Residuals vs. $\log p_2$.



(g) Residuals vs. $\log \sigma$.

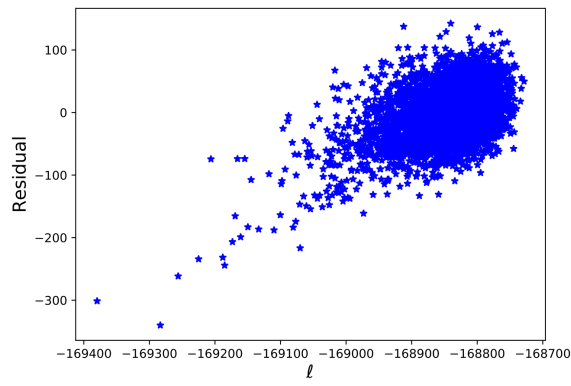


Figure 37: Residuals vs. $\hat{\ell}_{PF}$.

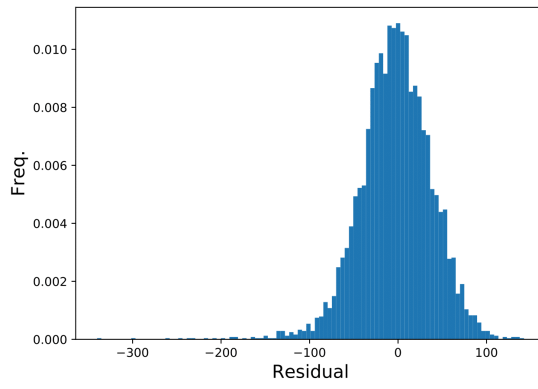


Figure 38: Histogram of residuals.

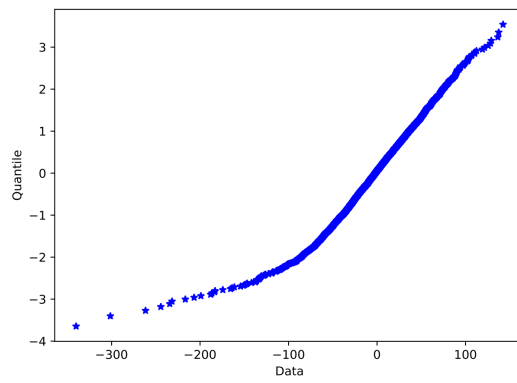


Figure 39: Normal probability plot for residuals.